

## Berberine represses $\beta$ -catenin translation involving 4E-BPs in hepatocellular carcinoma cells

Kanchan Vishnoi<sup>1, §</sup>, Rong Ke<sup>1, §</sup>, Karan S Saini<sup>1</sup>, Navin Viswakarma<sup>1</sup>, Rakesh Sathish Nair<sup>1</sup>,  
Subhasis Das<sup>1, 2</sup>, Zhengjia Chen<sup>3, 4</sup>, Ajay Rana<sup>1, 2, 5</sup>, Basabi Rana<sup>1, 2, 5</sup>

<sup>1</sup>Department of Surgery, Division of Surgical Oncology, University of Illinois at Chicago,  
Chicago, IL-60612, USA

<sup>2</sup>University of Illinois Hospital and Health Sciences System Cancer Center, University of Illinois  
at Chicago, Chicago, IL-60612, USA

<sup>3</sup>Division of Epidemiology and Biostatistics, School of Public Health, University of Illinois at  
Chicago, Chicago, IL 60612.

<sup>4</sup>Biostatistics Shared Resource Core, University of Illinois Cancer Institute, Chicago, IL  
60612.

<sup>5</sup>Jesse Brown VA Medical Center, Chicago, IL-60612, USA

<sup>§</sup> These authors contributed equally to this work

**Running Title:** Berberine represses  $\beta$ -catenin translation

**Corresponding Author:** Basabi Rana, Department of Surgery, Division of Surgical Oncology, University of Illinois at Chicago, Clinical Sciences Building, MC 958, Rm. 638, 840 S. Wood Street, Chicago IL 60612, USA. Tel.: 312-996-1078; Fax: 312-996-9365; E-mail: [basrana@uic.edu](mailto:basrana@uic.edu).

**Keywords:** berberine,  $\beta$ -catenin, mTOR, cap-dependent translation, eIF4E-binding protein (4E-BP), hepatocellular carcinoma, WNT signaling, AMP-activated protein kinase

Number of Pages: 45

Number of Tables: 0

Number of Figures: 9

Number of References: 75

Number of words in the abstract: 248

Number of words in the introduction: 694

Number of words in the discussion: 1,578

**Abbreviations:**

AMPK: AMP-activated protein kinase; BBR: Berberine; CC3, 8, 9: Cleaved caspases 3, 8, 9; 4E-BP: eIF4E-binding protein; HCC: Hepatocellular carcinoma; mTOR: Mammalian Target of Rapamycin; PARP: Poly (ADP-ribose) Polymerase; siRNA: Small Interference RNA.

## Abstract

Aberrant activation of Wnt/ $\beta$ -catenin axis occurs in several gastrointestinal malignancies due to inactivating mutations of APC (in colorectal cancer) or activating mutations of  $\beta$ -catenin itself (in hepatocellular carcinoma [HCC]). These lead to  $\beta$ -catenin stabilization, increase in  $\beta$ -catenin/TCF-mediated transcriptional activation and target gene expression, many of which are involved in tumor progression. While studying pharmaceutical agents that can target  $\beta$ -catenin in cancer cells, we observed that the plant compound berberine (BBR), a potent activator of AMP-activated protein kinase (AMPK), can reduce  $\beta$ -catenin expression and downstream signaling in HCC cells in a dose dependent manner. More in-depth analyses to understand the mechanism revealed that BBR-induced reduction of  $\beta$ -catenin occurs independently of AMPK activation, and does-not involve transcriptional or post-translational mechanisms. Pretreatment with protein synthesis inhibitor Cycloheximide antagonized BBR-induced  $\beta$ -catenin reduction, suggesting that BBR affects  $\beta$ -catenin translation. BBR treatment also antagonized mTOR activity, and was associated with increased recruitment of eIF4E-binding protein 1 (4E-BP1) in the translational complex, as revealed by m7-cap-binding assays, suggesting inhibition of cap-dependent translation. Interestingly, knocking down 4E-BP1 and -2 significantly attenuated BBR-induced reduction of  $\beta$ -catenin levels and expression of its downstream target genes. Moreover, cells with 4E-BP knockdown were resistant to BBR-induced cell death, and were re-sensitized to BBR following pharmacological inhibition of  $\beta$ -catenin. Our findings indicate that BBR antagonizes  $\beta$ -catenin pathway by inhibiting  $\beta$ -catenin translation and mTOR activity and thereby reduces HCC cell survival. These also suggest that BBR could be utilized for targeting HCCs that express mutated/activated  $\beta$ -catenin variants that are currently undruggable.

### **Significance Statement:**

$\beta$ -catenin signaling is aberrantly activated in different gastrointestinal cancers, including HCC, which is currently undruggable. In this study we describe a novel mechanism of targeting  $\beta$ -catenin translation via utilizing a plant compound BBR. Our findings provide a new avenue of targeting  $\beta$ -catenin axis in cancer, which can be utilized towards the designing of effective therapeutic strategies to combat  $\beta$ -catenin-dependent cancers.

## Introduction

Hepatocellular carcinoma (HCC) is one of the most common forms of gastrointestinal cancers, and a major cause of cancer-related death, worldwide (Torre et al., 2015). A vast majority of HCCs develop in the setting of chronic liver diseases and cirrhosis. The first line FDA-approved therapy available for treating advanced, unresectable HCC is the multikinase inhibitor Sorafenib, which despite some promising results (Llovet et al., 2008) is only effective for a few months. More recently, immune checkpoint inhibitors (nivolumab and pembrolizumab), several other multikinase inhibitors (lenvatinib, cabozantinib, regorafenib), and human monoclonal antibodies (ramucirumab) have been approved as first- or second-line therapies for advanced HCC (Caruso et al., 2020), (Pinyol et al., 2019). Despite this, the overall survival of patients is still not significantly improved, due to resistance. Newer and more effective therapeutic approaches are necessary for combating this deadly malignancy (Llovet and Bruix, 2008), (Porta and Paglino, 2010).

Among various pro-oncogenic pathways that are aberrantly activated in HCC, Wnt/ $\beta$ -catenin signaling cascade is specifically important. About 18.5% of HCCs harbor oncogenic mutations of  $\beta$ -catenin gene (*CTNNB1*) (de La Coste et al., 1998), (Miyoshi et al., 1998), (Perugorria et al., 2019), (Russell and Monga, 2018) leading to its activation (Nhieu et al., 1999). This scenario is much higher in hepatoblastomas, which harbor >50% *CTNNB1* mutations. Mutations of APC or  $\beta$ -catenin itself (Nhieu et al., 1999), (Morin et al., 1997) or activation of Wnt signaling results in stabilization of  $\beta$ -catenin (de La Coste et al., 1998), (Korinek et al., 1997), with increased nuclear translocation, interaction with transcription factors of the T cell factor/lymphoid enhancer factor

(TCF/LEF) family, and induction of target gene transcription (Bienz and Clevers, 2000), (Cadoret et al., 2002), which include cyclin D1, c-myc, MMP7, VEGF, Bcl-xL, Survivin, Glutamine Synthetase (Perugorria et al., 2019), (Vlad et al., 2008). Several inhibitors that can antagonize key steps of  $\beta$ -catenin/TCF axis have been developed, but none became successful clinically, although some clinical trials are currently ongoing to test the efficacy of Wnt antagonists on various liver diseases (Perugorria et al., 2019).

BBR, an alkaloid extracted from herbal plants, has been used in ancient Chinese medicine for a long time to treat microbial infections, diarrhea, which also possesses anti-diabetic (Yin et al., 2008), (Zhang et al., 2010) and cholesterol-lowering effects (Kong et al., 2004), (Krishan et al., 2015). In addition, various studies have shown antineoplastic properties of BBR in various cancers, such as colon, gastric, breast (Zhang et al., 2013), (Eom et al., 2008), (Kim et al., 2013), (Tillhon et al., 2012), (Wang et al., 2013) and others including HCC (Tsang et al., 2015), (Huang et al., 2018). Despite these, the detailed in-depth mechanism how BBR antagonizes pro-oncogenic pathways in various cancers is still unclear. BBR is also an activator of AMPK (Hawley et al., 2010), and some reports suggest that the antineoplastic effects of BBR are linked with AMPK activation (Kim et al., 2012), (Park et al., 2012), (Yu et al., 2014), (Li et al., 2015). Other studies however, have shown antagonism of  $\beta$ -catenin pathway as a potential mechanism (Wu et al., 2012), (Albring et al., 2013). A more recent study has shown that BBR can antagonize Wnt/ $\beta$ -catenin axis in colon cancer, via inducing  $\beta$ -catenin proteasomal degradation involving Retinoid X Receptor  $\alpha$  (Ruan et al., 2017).

Since  $\beta$ -catenin is a major pro-oncogenic axis in HCC and with no effective pharmaceutical options being available yet, the current studies were undertaken to determine whether BBR antagonizes  $\beta$ -catenin signaling in HCC, and to elucidate the underlying mechanism. Our studies revealed that BBR can antagonize  $\beta$ -catenin and its downstream signaling in HCC, in an AMPK-independent manner. Instead, this involved a novel, translational regulation via 4E-BP1 and 4E-BP2, which are known inhibitors of cap-dependent translation. Treatment with BBR antagonized mammalian target of rapamycin (mTOR) activity associated with reduced p4E-BP1<sup>Thr37/46</sup> levels and promoted interaction between eIF4E with 4E-BP1. Knocking down 4E-BP1 and 2 significantly attenuated BBR-induced reduction of  $\beta$ -catenin expression and downstream signaling. In addition, cells with 4E-BP1 and 2 knockdown were resistant towards BBR-induced cell death, which were re-sensitized by pharmacological targeting of  $\beta$ -catenin with iCRT-14. Taken together, these studies reveal a novel translational regulation of  $\beta$ -catenin, which contributes towards BBR-induced HCC cell death.

## Materials and Methods

### Reagents and Antibodies

DMEM, DMEM/F12, MEM and Opti-MEM media, TRIzol, RNase solution and Lipofectamine 2000 were purchased from Invitrogen (Carlsbad, CA); Berberine from Sigma (St. Louis, MO), luciferase assay reagent was from Promega (Madison, WI), Actinomycin D, iCRT-14 from Tocris (Minneapolis, MN), Lactacystin, MG-132 and cycloheximide from Millipore Sigma (Burlington, MA), 4EGI-1 from Selleckchem (Houston, TX), immobilized r-Aminophenyl-m7-GTP (C10-spacer) agarose beads from Jena Science (Jenna, Germany), Propidium Iodide (PI) and FITC Annexin V Apoptosis Detection Kit from BD Biosciences (San Jose, CA), JC-1 dye

and Rhodamine Phalloidin from Thermo-Fisher Scientific (Waltham MA). The antibodies utilized were obtained from the following sources: poly (ADP-ribose) polymerase (PARP), caspase-3, caspase 8, caspase 9, pAMPK<sup>T172</sup>, total AMPK, AMPK $\alpha$ 1 and  $\alpha$ 2, p $\beta$ -catenin<sup>Ser33/37/Thr41</sup>, cyclin D1, Axin2, c-Myc, p4E-BP1<sup>Thr37/46</sup>, 4E-BP1, 4E-BP2, p-p70S6K<sup>Thr389</sup>, p70S6K, pAKT<sup>Ser473</sup>, AKT, pGSK $\beta$ <sup>Ser9</sup>, GSK $\beta$ , pEIF4E<sup>Ser209</sup>, eIF4E, eIF4G1, eIF4G, cytochrome c, pACC<sup>Ser79</sup>, ACC from Cell Signaling Technologies (Danvers, MA),  $\beta$ -catenin from BD Transduction Laboratories, COX IV from abcam (Cambridge MA), GAPDH from Ambion Inc. (Austin, TX).

### Cell Culture

HCC cells (Hep3B, HepG2) and HEK293 were obtained from ATCC and Huh7 cells were obtained as described (Senthivinayagam et al., 2009), (Sureau et al., 1992). Hep3B and HepG2 cells were maintained in MEM media supplemented with 10% FBS, 1% Pen/Strep, 1% HEPES, 1% sodium pyruvate and 1% non-essential amino acids, Huh7 cells were maintained in DMEM/F12 media with 10% FBS and 1% Pen/Strep and HEK293 cells were maintained in DMEM media with 10% FBS and 1% Pen/Strep. In BBR-related experiments, cells were treated with 50 $\mu$ M BBR (unless indicated otherwise) for 16-24 hrs followed by Western blot or qPCR analyses.

### Preparation of Wnt3a-conditioned medium (CM)

L-Wnt3A (ATCC® CRL2647™) cells and L Cells (ATCC® CRL-2648™) were obtained from ATCC to prepare Wnt3a and control conditioned media respectively as per manufacturer's instructions. Cells were cultured in DMEM media supplemented with 10% FBS and 0.4mg/ml



G-418 for L-wnt3a cells and 1% Pen/strep for L-cells. For Wnt3a-CM, cells were split in the ratio of 1:10 in 10ml of DMEM media without G-418 in 10cm dish and allowed to grow. After 4 days, the first batch of CM was collected and another 10ml of fresh media was added to the cells. The second batch of CM was collected after 3 days and cells discarded thereafter. CM from two batches were mixed at 1:1 ratio, filtered using 0.22 $\mu$ m filter and stored at -20°C. Similarly, control CM was prepared by culturing L cells in DMEM with 10% FBS and 1%Pen/strep.

#### RNA Isolation and Quantitative Polymerase Chain Reaction (qPCR) Analysis

qPCR analysis was performed as described earlier (Viswakarma et al., 2017), (Ke et al., 2018). Briefly, total RNA was extracted from HCC cells treated with vehicle (DMSO) or BBR using TRIzol reagent and the integrity of 18S and 28S ribosomal RNA assessed by gel electrophoresis. cDNA synthesis was then performed using Superscript III First-Strand Synthesis System kit (Invitrogen, Carlsbad, CA) and amplified using SYBR Green PCR Master Mix (Applied Biosystems) in ABI StepOnePlus detection system (Applied Biosystems). The PCR cycling condition was set as: an initial denaturation step at 95°C for 2 min, 40 cycles at 95°C for 15 seconds, 60°C for 1 minute finally subjecting to melting temperature to check amplification curve. The relative changes in gene expression were estimated using the 2 $^{-\Delta\Delta C_t}$  method using 18S rRNA as a housekeeping gene. The lists of primers used are included in Supplementary Table S1.

#### Transient transfection and Luciferase Assays

Subconfluent populations of cells were transiently transfected using Lipofectamine-2000, with  $\beta$ -catenin/TCF-responsive luciferase-reporter construct (pGL3-OT) or the corresponding mutant

construct (pGL3-OF) along with  $\beta$ -galactosidase ( $\beta$ -gal) vector in the presence of empty vector or  $\beta$ -catenin-expressing vector as reported earlier (Thylur et al., 2011).  $\beta$ -catenin/TCF transcriptional activity was assessed using luciferase reporters containing TCF sites linked to luciferase reporter (pGL3-OT) and compared with a control reporter (pGL3-OF), where the TCF sites were mutated. These reporter constructs were derived from the TOPFLASH and FOPFLASH vectors respectively, and obtained from Dr. Bert Vogelstein (Morin et al., 1996), (Korinek et al., 1997), (Shih et al., 2000). Treatment with vehicle or BBR was initiated after 48hrs of transfection and luciferase and  $\beta$ -galactosidase ( $\beta$ -gal) assays were performed using a luminometer (Berthold Technologies, TriStar<sup>2</sup> LB 942) and a microplate reader (BioTek, EPOCH2), respectively. Each transfection was performed in triplicate, and each experiment was repeated at least twice. The results obtained were calculated as the ratio of relative light units (RLU) to  $\beta$ -gal values. For the luciferase assays with AMPK $\alpha$ 1 or AMPK $\alpha$ 2 knockdown, cells were co-transfected as above in the presence of control-siRNA, AMPK $\alpha$ 1-siRNA, AMPK $\alpha$ 2-siRNA or AMPK $\alpha$ 1+2-siRNA and analyzed as above.

#### Small Interference RNA (siRNA)

siRNA smart pool against hAMPK $\alpha$ 1 (Cat # L-005027-00), hAMPK $\alpha$ 2 (Cat # L-005361-00), were purchased from Dharmacon (Lafayette, CO). A negative control siRNA from Ambion Inc. (Austin, TX) was used as control siRNA. siRNA transfection was performed using Lipofectamine 2000 as per the manufacturer's instructions and as described previously (Santha et al., 2015). Briefly, subconfluent cells plated in 35mm plates were transfected with 50nM of either control siRNA or target siRNA for 24 hrs followed by recovery in serum containing

medium. The transfected cells were treated after 48-72 hrs of transfection with either DMSO or BBR for an additional 16 hrs followed by western blot analysis.

### Stable cell line creation

Lentiviral particles containing human AMPK $\alpha$ 1/2-shRNA (sc-45312-V) obtained from Santa Cruz Biotechnology was used to knockdown endogenous AMPK $\alpha$ 1/2 expressions, following manufacturer's protocol and as reported (Laderoute et al., 2014). A control lentiviral preparation encoding a scrambled shRNA sequence (sc-108080) was used as negative control. Briefly, subconfluent HCC cells plated in 12-well plates were transduced overnight with lentiviral particles (~ 40,000-80,000 Infectious Unit) in complete medium containing Polybrene (5 $\mu$ g/ml), followed by selection in puromycin-containing medium. Puromycin-resistant colonies were propagated, stored and the degree of knockdown was determined by western blot analysis.

For creating the eIF4E-BP1 and eIF4E-BP2 knockdown stable cells, we utilized pLKO.1-CMV-puro-eIF4E-BP1-shRNA (TRCN0000040203) and pLKO.1-CMV-neo-eIF4EBP2-shRNA (TRCN0000117814) lentiviral constructs from Sigma. Lentiviral particles were produced as described earlier (Das et al., 2019) by co-transfecting HEK293 FT cells (Life Technologies, USA) with either one of the lentiviral plasmids along with psPAX2 and pMD2G packaging plasmids using Lipofectamine 2000. Titrations were performed first to achieve an MOI of 0.3 to 0.5 and the infection efficiency confirmed by western blots. Huh7 cells were then transduced with the lentiviral particles as described above and stable cells lines were selected using both puromycin (for eIF4E-BP1 shRNA) and neomycin (for eIF4EBP2 shRNA).

### Cap-binding affinity assay

Cap-binding affinity assay was performed as described (Zhan et al., 2015) with modifications. Briefly, cells treated with vehicle or BBR were lysed in NP-40 lysis buffer (20mM Tris-HCl pH 8.0, 150mM NaCl, 2mM EGTA pH 8.0, 10% Glycerol, 1% NP-40, 50mM  $\beta$ -glycero phosphate, 1mM Na-orthovanadate, 1mM dithiothreitol, 1mM phenylmethylsulfonyl fluoride containing a mixture of proteinase inhibitors). Equal amounts of protein extracts were then added to the  $m^7$ GTP agarose beads (30 $\mu$ l) and incubated on a rotator for 3 hours at 4 degrees, followed by washing with NP40 lysis buffer for 4 times.  $m^7$ GTP-bound proteins were then analyzed by western blots.

### Apoptosis assay

Apoptosis assay was performed using FITC Annexin V Apoptosis Detection Kit (BD Biosciences) as per manufacturer's instructions. Cells seeded at a density of  $1.5 \times 10^6$  cells/plate in 35mm plates were treated with BBR, iCRT alone or in combination for various lengths of time. At the time of harvest, they were trypsinized and distributed equally into two parts: one part was used for apoptosis assay and the other part for JC-1 assay (described below). Cells for apoptosis assay were centrifuged at 2000 rpm for 5 min, washed once with ice-cold PBS and once with 1X binding buffer, followed by re-suspension in 100 $\mu$ l 1X binding buffer and incubation with 5 $\mu$ l each of Annexin V and PI at room temperature in dark for 15 minutes. 400 $\mu$ l of 1X binding buffer was then added to each sample and apoptosis assays performed using Gallios flow cytometer (Beckman Coulter). The data was analyzed using FlowJo software.

### JC-1 assay

To determine changes in mitochondrial membrane potential, a distinctive feature of early apoptosis, JC-1 assay was performed as per manufacturer's instructions. Cells harvested as above were suspended in 1ml of warm growth media, followed by incubation in 2 $\mu$ M JC-1 dye at 37°C, 5% CO<sub>2</sub> in incubator for 15min. Cells were then washed twice with PBS, resuspended in 500 $\mu$ l of PBS and readings acquired on Gallios flow cytometer (Beckman Coulter) using 488 nm laser. JC-1 red emission of healthy mitochondria was obtained at 590nm and the green emission of apoptotic mitochondria (with reduced membrane potential) at 530nm. The data was analyzed using FlowJo software.

### Cell-cycle analysis

Cells seeded at a density of 0.6 x 10<sup>6</sup>/plate in 35mm plates were treated with BBR for different lengths of time. At the time of harvest, they were washed in PBS, fixed in ice-cold 70% ethanol and stored at -20°C overnight. Next day, the fixed cells were washed twice with PBS and treated with 50 $\mu$ l of RNase at room temperature (stock 100 $\mu$ g/ml). After 15min, 200 $\mu$ l of PI (Stock 50 $\mu$ g/ml) was added and cell-cycle analysis was performed using Gallios flow cytometer (Beckman Coulter). The data was analyzed using FlowJo software.

### Migration assay

The effect of BBR on the cell migration was determined using the ORIS™ cell migration assay kit (Platypus, NJ, USA). The ORIS cell migration assay was performed using a 96-well plate, where a 'stopper' barrier was used to create a central cell-free detection zone for cells to migrate. Briefly, cells at a density of 10,000 cells/well (in quadruplicate) were added to each well through

wedge of the stopper and allowed to grow overnight. Next day, the stoppers were removed, cells were washed with media and treated with DMSO or BBR. The readings were taken by Celligo Imaging Cytometer (Nexcelom Bioscience, MA, USA) after 48h of BBR treatment. Amount of cells migrated into the central migration zone was used to calculate percent increase in migration.

#### Detection of cytochrome *c* release

To detect cytochrome *c* release from mitochondria to cytoplasm, cells were separated into cytoplasmic and mitochondrial fractions as described with modifications (Chandra et al., 2004). For cytoplasmic and mitochondrial fractionation, cells washed with PBS were re-suspended in homogenization buffer (20mM HEPES pH 7.5, 10mM KCl, 1.5mM MgCl<sub>2</sub>, 1mM EDTA, 1mM EGTA, 1mM DTT, 250mM Sucrose) and incubated on ice for 30min with intermittent mixing. Cells were then homogenized (with 10-12 strokes) in cold and the homogenate was centrifuged at 1,000 rpm for 5min at 4°C, to remove nuclei, cellular debris and intact cells. The resultant supernatant was collected and centrifuged at 12,000 rpm for 20min at 4°C to separate cytoplasmic fraction (as supernatant) and mitochondrial fraction (as pellet). The cytoplasmic protein extracts were preserved and mitochondrial pellet was washed with homogenizing buffer twice at 12,000 rpm for 10min each at 4°C. The mitochondrial pellets were resuspended in mitochondrial protein extraction buffer (50mM Tris-HCl, pH 7.4, 150mM NaCl, 2mM EDTA, 2mM EGTA, 0.2% Triton X 100, 0.3% NP-40, 2.5mM PMSF and protease inhibitor cocktail). Following incubation on ice for 10min, they were centrifuged at 12,000 rpm for 20min at 4°C, mitochondrial proteins were collected as supernatant and preserved. Both cytoplasmic and

mitochondrial proteins were boiled and denatured using Laemmli buffer and used for western blotting.

### Western Blot Analysis

Western blot analysis was performed following procedures described previously (Mishra et al., 2010), (Pradeep et al., 2004). Briefly, equal amounts of total cell extracts were fractionated by SDS-PAGE, transferred to PVDF membranes, and subjected to Western blot analysis utilizing various antibodies. The bar graphs for most proteins represent the ratio of the respective protein/GAPDH, and those for pAMPK represent the ratio of pAMPK/total AMPK.

### Statistical analyses

All data were presented as means with  $\pm$  S.D. For determining significance between control (vehicle) and BBR-treated samples, Student's t-test was performed and expressed as \*  $P \leq 0.05$ , \*\*  $P \leq 0.01$ , \*\*\*  $P \leq 0.001$ , \*\*\*\*  $P \leq 0.0001$ , ns:  $P > 0.05$  not significant. The data of Supplementary Table S2 were presented either as mean of the group with its 95% confidence interval (CI), or for the key comparisons, the difference of means between pairwise groups together with 95% CI of the difference using the pooled standard error. Two or three-way ANOVA were employed to test the significance of treatment group, vehicle type, or time. To control the overall type I error at 0.05 for multiple tests, the Tukey's followup tests were used for the pairwise comparisons and Dunnett's tests were used instead to compare each mean to the control mean. The results of ANOVA, 95% CI of difference, Tukey's test and Dunnett's test have been summarized in Supplementary Table S2.

## Results

BBR antagonizes  $\beta$ -catenin pathway in HCC cells: In an attempt to identify pharmacological agents that can effectively target  $\beta$ -catenin, we determined the effect of BBR on  $\beta$ -catenin axis in HCC. Treatment of HCC cells (Huh7 and Hep3B) with BBR showed a dose and time-dependent reduction of  $\beta$ -catenin (Figs 1A, B, C), suggesting an antagonism of this pathway. Interestingly, BBR treatment also reduced the expression of mutated  $\beta$ -catenin in the HepG2 cells (Fig 1D), which is resistant to degradation via conventional APC/GSK3 $\beta$  pathway. Treatment of HEK293 cells with BBR also showed a dose-dependent reduction of  $\beta$ -catenin expression (Fig supplementary Fig S1A). To determine whether BBR can antagonize  $\beta$ -catenin/TCF transcriptional activity and downstream target gene expression, luciferase assays were performed with  $\beta$ -catenin/TCF-responsive reporter (pGL3-OT) and the corresponding mutant (pGL3-OF) as reported (Thylur et al., 2011). BBR suppressed OT-reporter activity in a dose-dependent manner (Figs 2A, B) and antagonized  $\beta$ -catenin target gene (Fig 2D), and protein expression (Figs 2C, S1B). These observations suggested that BBR might be an effective therapeutic approach to target  $\beta$ -catenin in HCCs.

BBR regulates  $\beta$ -catenin pathway independent of AMPK: Our earlier studies showed that BBR and TRAIL combination-induced apoptosis is mediated via AMPK activation (Ke et al., 2018). BBR-induced activation of AMPK has been reported by others as well (Lee et al., 2006). Treatment with BBR also showed an increase in pAMPK<sup>T172</sup> levels, suggesting its activation mostly, during the time of  $\beta$ -catenin reduction (Figs 1A-D and S1A-B). The reduction of pAMPK<sup>T172</sup> observed with BBR at 24hrs is most likely due to a reduction of total AMPK expression, as suggested by the bar graphs of pAMPK/AMPK (Fig 1A, lanes 7, 8). Results from



this study on BBR-induced activation of AMPK are consistent with previous findings (Hawley et al., 2010), (Li et al., 2015). To determine whether AMPK was involved in BBR-induced antagonism of  $\beta$ -catenin, AMPK $\alpha$ 1 and  $\alpha$ 2 levels were transiently knocked down using corresponding siRNAs. Surprisingly, knocking down AMPK $\alpha$  was unable to restore  $\beta$ -catenin expression, in the presence of BBR (Figs 3A and S2A). To confirm this further, HCC cells with stable AMPK $\alpha$ 1,  $\alpha$ 2 knockdown were generated, which also showed BBR-induced reduction of  $\beta$ -catenin in the absence of AMPK  $\alpha$ 1,  $\alpha$ 2 (Figs 3B, 3C). Similarly, BBR reduced expression of  $\beta$ -catenin target proteins (cyclin D1 and Axin2) even with AMPK  $\alpha$ 1,  $\alpha$ 2 knockdown (Fig 3C). Furthermore, luciferase assays showed that BBR was capable of reducing OT-luc activity in the absence of AMPK  $\alpha$ 1,  $\alpha$ 2 (Figs 3D and S2B). In addition, treatment with various AMPK agonists although activated AMPK pathway (Lin et al., 2017), were unable to reduce  $\beta$ -catenin expression in each case (Fig S2C, compare  $\beta$ -catenin and pACC in DMSO, BBR, salicylate, A769662). These suggested that BBR can reduce  $\beta$ -catenin expression and antagonize its downstream signaling in an AMPK-independent manner.

*BBR regulates  $\beta$ -catenin expression at the level of translation:* We next focused on determining whether BBR-induced reduction of  $\beta$ -catenin was at the level of transcription, translation or post-translation. Recently, BBR was shown to target  $\beta$ -catenin post-translationally via a proteasome-dependent pathway in colon cancer cells (Ruan et al., 2017). Estimation of  $\beta$ -catenin mRNA expression with and without BBR treatment showed no significant difference (Fig 4A), at a time when protein expression was reduced significantly (Fig 1A). In addition, BBR was able to reduce  $\beta$ -catenin expression even in the presence of an inhibitor of transcription, Actinomycin D (Fig 4B), suggesting this was regulated independent of transcription. To determine the possibility of a

post-translational regulation mediated via proteasomes, cells were pretreated with two different proteasomal inhibitors Lactacystin and MG132 (Alao et al., 2006), which were unable to rescue  $\beta$ -catenin expression following BBR treatment (Figs 4C, D). Furthermore, the levels of p $\beta$ -catenin<sup>Ser33/37/Thr41</sup> were also reduced with BBR treatment (Figs S3A, B), and correlated with an increase in pGSK3 $\beta$ <sup>Ser9</sup> levels (indicating inhibition) under these conditions (Figs 5A, B), suggesting BBR does-not significantly regulate post-translational modification of  $\beta$ -catenin. Taken together, these suggested the possibility that BBR might target  $\beta$ -catenin at the level of translation. To explore this possibility cells were pretreated with translational inhibitor cycloheximide (CHX) prior to BBR treatment. Interestingly, BBR was unable to reduce  $\beta$ -catenin expression in the presence of CHX pretreatment (Fig 4E, compare lanes 4&5 with 7&8), suggesting BBR-induced reduction involves a translational regulation. It is unclear at this time why treatment with CHX and BBR did not show the regular decay of  $\beta$ -catenin observed under CHX-DMSO conditions (lanes 3-5), indicating additional mechanisms. The mostly likely explanation is that CHX also inhibited translation of those that mediate  $\beta$ -catenin degradation including those involved in proteasomal pathway. To rule out the proteasomal pathway involvement, we have performed studies with two different proteasomal inhibitors (Lactacystin and MG132), which were unable to reverse BBR-induced  $\beta$ -catenin reduction (Figs 4C, D).

*BBR inhibits mTOR pathway and cap-dependent translation:* Regulation of  $\beta$ -catenin expression via cap-dependent translation have been reported earlier. The proto-oncogene c-Src was shown to induce  $\beta$ -catenin levels via cap-dependent translation (Karni et al., 2005) and MAP Kinase interacting serine/threonine kinase (MNK)-eukaryotic translation initiation factor 4E (eIF4E) axis was shown to regulate increased  $\beta$ -catenin translation and activity (Lim et al., 2013). Since

mTOR is a positive regulator of cap-dependent translation (Ma and Blenis, 2009), we first detected the effect of BBR on mTOR activation. HCC cells treated with BBR showed that BBR can inhibit p-p70S6K<sup>Thr389</sup> and p4EBP1<sup>Thr37/46</sup> levels in a time-dependent manner (Figs 5A, B), suggesting inhibition of mTORC1 axis. In addition, BBR also showed increase in pAKT<sup>Ser473</sup> and its downstream pGSK3 $\beta$ <sup>Ser9</sup> levels, likely due to a corresponding activation of mTORC2. The levels of p-eIF4E<sup>Ser209</sup> also was reduced with BBR treatment (Figs 5A, B), which is known to be phosphorylated by MNKs. Taken together, these suggested a potential inhibition of cap-dependent translation when treated with BBR due to inhibition of mTORC1 and eIF4E phosphorylation. In fact, m7-GTP pulldown assays performed with BBR-treated extracts showed increased recruitment of 4EBP1 and a corresponding reduction of eIF4G in the translation complex when treated with increasing dose of BBR (Fig 5C, D).

BBR antagonizes  $\beta$ -catenin pathway via targeting cap-dependent translation: Since BBR antagonized cap-dependent translation, we determined next whether BBR reduced  $\beta$ -catenin expression via targeting cap-dependent translation. Treatment with 4EGI-1, a small molecule that inhibits interaction between initiation factors eIF4E and eIF4G (Moerke et al., 2007) reduced  $\beta$ -catenin expression to very low levels almost similar to BBR (Fig 6A, compare lanes 1&5). Interestingly, using HepG2 cells (which expresses a degradation-resistant truncated form of  $\beta$ -catenin), we determined that BBR as well as 4EGI-1 reduced expression of full length and truncated  $\beta$ -catenin and its downstream targets (Fig 6B). These suggested that in HCC cells mutated  $\beta$ -catenin expression can be targeted by 4EGI-1. To validate this further, stable HCC cells overexpressing either scrambled shRNA (control-shRNA) or 4EBP1 and 2 shRNA (4EBP1+2-shRNA) were generated, which showed a significant reduction of 4EBPs in the

4EBP1+2 shRNA cells (Fig 6C). Interestingly, treatment with BBR showed reduction of  $\beta$ -catenin expression in the control-shRNA cells, while BBR was unable to reduce it in the 4EBP1,2-shRNA cells (Fig 6C), thus suggesting that BBR-induced reduction of  $\beta$ -catenin expression involves antagonism of cap-dependent translation via 4EBPs. BBR treatment was also unable to reduce wnt3a-induced  $\beta$ -catenin/TCF transcriptional activity in the 4EBP1+2-shRNA cells, while it effectively antagonized this in control-shRNA cells (Figs S4A, S4B). Further analysis performed to estimate changes in  $\beta$ -catenin downstream target gene expressions showed that BBR was unable to reduce these levels in 4EBP1+2-shRNA cells (Figs 6D, 6E, S5A, S5B). Taken together these confirmed that BBR can antagonize  $\beta$ -catenin expression and downstream signaling via targeting cap-dependent translation.

*BBR induces HCC cell apoptosis via antagonizing cap-dependent translation and  $\beta$ -catenin axis:*

To determine which of the biological effects of BBR in HCC are mediated via inhibition of cap-dependent translation, we focused on the effects of BBR on cell proliferation, migration and apoptosis. As shown in Fig S6A, S6B, although BBR can induce cell cycle arrest in these cells (increase in G2/M stage), knocking down 4EBP1, 2 was unable to reverse this. Similarly, BBR-reduction of migration was not rescued with 4EBP1, 2 knockdown (Fig S6C), suggesting BBR-induced cell cycle arrest and inhibition of migration likely to be independent of cap-dependent translation. To determine the effects on cell death, apoptosis assays were designed first following treatment of HCC cells with BBR. These showed an increase in cellular apoptosis and mitochondrial damage by BBR in a time and dose-dependent manner in Huh-7 (Figs S7A, B, C) and Hep3B cells (Figs S8A, B, C). Interestingly, similar apoptosis assays carried out with BBR showed that knocking down 4EBP1 and 2 significantly attenuates BBR-induced apoptosis and

mitochondrial damage (Fig 7A, B), while high level apoptosis was observed in the control-shRNA cells. Similarly, western blot analysis revealed that BBR-induced poly (ADP-ribose) polymerase (PARP) and caspase 3, 8, 9 cleavages involve antagonism of cap-dependent translation (Fig 7C).

Since BBR-induced apoptosis and antagonism of  $\beta$ -catenin pathway were both reversed with 4EBP1, 2 knockdown, we hypothesized that inhibiting  $\beta$ -catenin might re-sensitize these cells. To address this, we utilized iCRT-14 (iCRT), which disrupts  $\beta$ -catenin signaling by antagonizing  $\beta$ -catenin-TCF interaction (Gonsalves et al., 2011), (Watanabe and Dai, 2011). In fact, iCRT at a lower dose (10 $\mu$ M) inhibited  $\beta$ -catenin/TCF-responsive OT activity (Fig S9A), but not OF activity (Fig S9B). Interestingly, treating 4EBP1+2-shRNA cells with low dose of iCRT resulted in increased apoptosis with or without BBR, which seemed more pronounced than in the control-shRNA cells (Figs 8A, B, C). These suggested that in the absence of 4EBP1, 2, the cells become too addicted to  $\beta$ -catenin for survival and so antagonizing  $\beta$ -catenin by iCRT increases their susceptibility to BBR-induced cell death. Despite increased apoptosis, iCRT was unable to induce caspase 3 cleavage in the 4EBP1+2 shRNA cells (Fig S9C). Since iCRT-BBR combination increased mitochondrial damage (Figs 8B, C), it suggested the possibility of mitochondrial apoptosis cascade. In fact, treatment with iCRT and BBR promoted a significant increase in cytoplasmic cytochrome *c* release in the 4EBP1+2 shRNA cells (Fig 8D). Combined together, these studies reveal a novel translational control of  $\beta$ -catenin by BBR, which can be utilized to promote cell death in  $\beta$ -catenin-mutated HCCs involving intrinsic apoptotic pathway.

## Discussion

Identification of more effective therapeutic approaches that can antagonize  $\beta$ -catenin axis is critical for targeting aberrant  $\beta$ -catenin activation in HCCs. In an attempt to identify specific signaling pathways that can ameliorate TRAIL-resistance, we reported earlier that combination of TRAIL and Troglitazone can sensitize TRAIL-resistant cells towards apoptosis, that required the activation of AMPK (Senthivinayagam et al., 2009), (Santha et al., 2015). Interestingly, treatment with Troglitazone alone, also inhibited  $\beta$ -catenin and its downstream axis by an APC-independent mechanism (Sharma et al., 2004). More recently we observed that treatment with the natural compound BBR can significantly reduce HCC cell viability and induce apoptosis in combination with TRAIL, in an AMPK-dependent manner (Ke et al., 2018). In addition, BBR also showed antagonistic effects on  $\beta$ -catenin axis involving a novel mechanism, which is the focus of the current studies.

Earlier studies have shown that BBR can antagonize cancer progression, and this anticancer activity is linked with an antagonism of Wnt/ $\beta$ -catenin signaling (Wu et al., 2012), (Ruan et al., 2017). Despite this, the mechanism involved in  $\beta$ -catenin antagonism is largely unknown. Since  $\beta$ -catenin is often mutated and its downstream signaling activated in HCC, our goal here was to elucidate in detail the mechanism by which BBR antagonized  $\beta$ -catenin pathway in HCC. Our results demonstrated that BBR can inhibit  $\beta$ -catenin expression in various HCC cells in a dose and time-dependent manner. Interestingly, BBR also suppressed  $\beta$ -catenin levels in HepG2 cells, which express a truncated/mutated form of  $\beta$ -catenin that is resistant to conventional GSK3 $\beta$ /APC/Axin-mediated proteasomal degradation pathway.  $\beta$ -catenin is known to interact with TCF or LEF transcription factors which in turn activate target gene transcription (Molenaar

et al., 1996), (Behrens et al., 1996), (Huber et al., 1996). Thus, reduction of  $\beta$ -catenin expression is expected to reduce  $\beta$ -catenin/TCF-mediated transcriptional activity. In fact, BBR-induced reduction of  $\beta$ -catenin expression also antagonized  $\beta$ -catenin/TCF-mediated transcriptional activity and downstream signaling. These suggest that BBR (or its derivatives) might have the potential to be developed as therapeutic agents to target  $\beta$ -catenin-mutated HCCs. BBR is a known agonist of AMPK (Hawley et al., 2010), and earlier studies have established a link between BBR's antineoplastic effects with AMPK signaling (Kim et al., 2012), (Park et al., 2012), (Yu et al., 2014), (Li et al., 2015). A crosstalk of AMPK and  $\beta$ -catenin have also been reported (Zhao et al., 2010). BBR treatment in our studies showed an increase in pAMPK<sup>T172</sup> levels, which followed an inverse correlation with  $\beta$ -catenin reduction, suggesting the possibility of AMPK involvement. However, AMPK $\alpha$ 1 and 2 transient knockdown was unable to reverse BBR-induced reduction of  $\beta$ -catenin or downstream signaling. These were further validated by stable knockdown of AMPK $\alpha$ 1 and  $\alpha$ 2, thus confirming that BBR-induced antagonism of  $\beta$ -catenin signaling is independent of AMPK. These are consistent with earlier studies which showed that BBR could antagonize NF $\kappa$ B signaling in colon cancer via AMPK-independent mechanism (Li et al., 2015).

A recent study in colon cancer cells have demonstrated that BBR antagonizes  $\beta$ -catenin via promoting its proteasomal degradation involving RXR $\alpha$  (Ruan et al., 2017). However, in our studies, pretreatment with two different inhibitors of proteasomal degradation (Lactacystin and MG132), were unable to fully rescue  $\beta$ -catenin expression in the HCC cells. These data together with the observation that, BBR can reduce mutant  $\beta$ -catenin expression in the HepG2 cells (this mutant form is resistant towards degradation by proteasomal pathway), suggested the possibility

that BBR might target  $\beta$ -catenin via additional mechanisms. The likely explanation behind these discrepancies is that BBR-induced reduction of  $\beta$ -catenin in colon and liver cancer cells might be different. It is important to note, while APC mutations are found in colorectal cancer,  $\beta$ -catenin mutations are prevalent in liver cancer (Miyoshi et al., 1998), majority of which enable  $\beta$ -catenin to evade GSK3 $\beta$ /APC-induced proteasomal degradation. To elucidate this pathway further, we also determined that this antagonism of  $\beta$ -catenin is not at the level of mRNA expression, since it was reduced in the presence of Actinomycin D and  $\beta$ -catenin mRNA levels didn't show significant inhibition with BBR when protein levels were reduced. Interestingly, pretreatment with protein synthesis inhibitor cycloheximide almost completely antagonized BBR-induced  $\beta$ -catenin reduction. This suggested a very novel translational mechanism involved in BBR-induced reduction of  $\beta$ -catenin in HCC.

Translational regulation of  $\beta$ -catenin involving cap-dependent translation has been shown before. Activation of Src pathway induced  $\beta$ -catenin expression and its downstream transcriptional activity by promoting cap-dependent translation (Karni et al., 2005). Activation of eIF4E (an essential component of cap-dependent mRNA translation), can increase  $\beta$ -catenin mRNA translation and promote stem cell function in blast crisis chronic myeloid leukemia (Lim et al., 2013). Cap-dependent translation is promoted by mTORC1 via phosphorylation and inhibition of 4E-BPs (4E-BP1, 2, 3), leading to the association of eIF4E and eIF4G, formation of eIF4F and initiation of translation (Pause et al., 1994), (Haghighat et al., 1995). Inactivation of mTORC1 signaling will thus lead to activation of 4E-BPs and repression of cap-dependent translation. In addition to mTORC1, GSK3 $\beta$  (Shin et al., 2014b) and Casein Kinase 1 $\epsilon$  (Shin et al., 2014a) has also been shown to phosphorylate and inhibit 4E-BPs and promote cap-dependent translation.



Our results with BBR showed a time dependent inhibition of mTORC1, as indicated by reduced levels of p-p70S6K<sup>Thr389</sup> and p4E-BP1<sup>Thr37/46</sup>, two downstream targets of mTORC1 pathway. Our findings support earlier observations, which showed BBR-mediated antagonism of mTOR pathway (Wang et al., 2010). In addition, and likely due to activation of mTORC2 axis, BBR also increased pAKT<sup>S473</sup> and pGSK3 $\beta$ <sup>Ser9</sup> (indicating inhibition of GSK3 $\beta$  signaling) levels. Taken together, these suggest that BBR can reduce phosphorylation and activate 4E-BPs via two different mechanisms: one by inhibiting mTORC1 and second by inactivating GSK3 $\beta$ , thus setting the stage for inhibition of cap-dependent translation. In fact, m<sup>7</sup>GTP pulldown assays confirmed this, by showing that BBR treatment reduces the association of eIF4E with eIF4G, while increasing its association with 4E-BP1. To determine whether BBR reduced  $\beta$ -catenin via antagonizing cap-dependent translation, HCC cells with stable knockdown of 4E-BP1 and 2 (4EBP1+2 shRNA) were created. Interestingly, while treatment with BBR reduced  $\beta$ -catenin expression in the control-shRNA cells, it was completely unable to reduce this in the 4EBP1+2 shRNA cells. Similarly, BBR was unable to reduce the levels of  $\beta$ -catenin downstream targets in the 4EBP1+2 shRNA cells, confirming that BBR antagonizes  $\beta$ -catenin expression and downstream signaling via targeting cap-dependent translation. This is further validated by the fact that 4EGI-1 (inhibitor of translation) (Moerke et al., 2007), can decrease  $\beta$ -catenin expression and downstream signaling significantly even in the absence of BBR. The exact reason behind the increase of  $\beta$ -catenin with 4EGI-1 in the Huh7 cells (Fig 6A, lanes 7, 8) and not in other HCC cells (Fig 6B) is unclear, and might indicate cell-specific effects. Similar cancer cell specific effects of 4EGI-1 on c-myc translation was also reported in malignant pleural mesothelioma (De et al., 2018). In addition, under certain stress conditions translation of oncogenes can switch from cap-dependent translation to internal ribosome entry segment

(IRES)-dependent translation. This was observed with c-myc, whose translation is normally induced by cap-dependent mechanism downstream of mTOR pathway (West et al., 1998), but was induced by IRES-dependent pathway when cells underwent apoptosis (Stoneley et al., 2000). Similarly, translation of vascular endothelial growth factor is induced by IRES during hypoxia, when cap-dependent translation is inhibited (Stein et al., 1998). It is thus possible, that in certain cells, inhibition of  $\beta$ -catenin cap-dependent translation (by 4EGI-1) results in a switch towards cap-independent translation. To our knowledge, this is the first report to show that BBR in fact, antagonizes  $\beta$ -catenin axis in HCC via targeting cap-dependent translation. Further studies to determine the biological effects showed that BBR promoted cell death via antagonism of cap-dependent translation, since this process was significantly attenuated in 4EBP1+2 shRNA cells. Interestingly, pharmacological targeting of  $\beta$ -catenin/TCF-transcriptional activity by iCRT-14 (Gonsalves et al., 2011), (Watanabe and Dai, 2011) re-sensitized these cells to cell death with or without BBR, via increasing cytoplasmic cytochrome *c* release. Based on our current data and published results, we have proposed a model by which BBR regulates  $\beta$ -catenin translation and its impact on HCC cell survival/death (Fig 9).

In conclusion, our studies demonstrate a novel mechanism by which BBR inhibits  $\beta$ -catenin and its downstream signaling axis in HCC, involving inhibition of cap-dependent translation. This pathway also seems to mediate BBR-induced cell death involving cytoplasmic *c* release. Some limitations of the current study include the *in vitro* cellular approaches used, which needs to be validated *in vivo* utilizing animal models of HCC. However, BBR has been used in earlier *in vivo* studies without any reported toxicity, suggesting its potential to be developed as a cancer therapeutic agent (Ruan et al., 2017). Since  $\beta$ -catenin is often mutated in HCC patients, most of

which are resistant to degradation by conventional proteasomal pathway, BBR (or its derivatives) and other translation inhibitors (e.g. 4EGI-1) might provide a novel/alternate therapeutic axis by which these can be targeted. In addition, due to its antagonistic effects on GSK3 $\beta$  activity, BBR seems to provide a therapeutic opportunity for those cancers, which are dependent on aberrant GSK3 $\beta$  activation (Wilson and Baldwin, 2008), (Kotliarova et al., 2008). While the pharmacological effects of BBR on  $\beta$ -catenin pathway antagonism is quite remarkable, the oral bioavailability and hence druggability of BBR is currently low due to several reasons (Wang et al., 2018). Based on the current studies, combination of BBR with antagonists of  $\beta$ -catenin or inhibitors of cap-dependent translation might help overcoming the difficulty of high dose administration. In fact, a current Phase I trial with BBR combination showed promising results in patients with ulcerative colitis (Xu et al., 2020).

#### **Acknowledgement:**

We are grateful to Dr. Bert Vogelstein for providing the pGL3OT and pGL3OF luciferase reporters (Morin et al., 1996), (Korinek et al., 1997), (Shih et al., 2000). Research reported in this publication was supported in part by the University of Illinois Cancer Center Biostatistics Shared Resource Core (BSRC).

#### **Author Contributions:**

**Participated in Research Design:** Vishnoi, Ke, Saini, Viswakarma, Nair, Das, A.R and B.R.

**Conducted Experiments:** Vishnoi, Ke, Saini, Viswakarma, Nair and Das

**Performed Data Analysis:** Vishnoi, Ke, Saini, Viswakarma, Nair, Das, Chen, A.R and B.R.

**Wrote or contributed to the Writing of the Manuscript:** Vishnoi, Ke, A.R, and B.R.

## References:

- Alao JP, Stavropoulou AV, Lam EW, Coombes RC and Vigushin DM (2006) Histone deacetylase inhibitor, trichostatin A induces ubiquitin-dependent cyclin D1 degradation in MCF-7 breast cancer cells. *Mol Cancer* **5**: 8.
- Albring KF, Weidemuller J, Mittag S, Weiske J, Friedrich K, Geroni MC, Lombardi P and Huber O (2013) Berberine acts as a natural inhibitor of Wnt/beta-catenin signaling--identification of more active 13-arylalkyl derivatives. *Biofactors* **39**(6): 652-662.
- Behrens J, von Kries JP, Kuhl M, Bruhn L, Wedlich D, Grosschedl R and Birchmeier W (1996) Functional interaction of beta-catenin with the transcription factor LEF-1. *Nature* **382**(6592): 638-642.
- Bienz M and Clevers H (2000) Linking colorectal cancer to Wnt signaling. *Cell* **103**(2): 311-320.
- Cadoret A, Ovejero C, Terris B, Souil E, Levy L, Lamers WH, Kitajewski J, Kahn A and Perret C (2002) New targets of beta-catenin signaling in the liver are involved in the glutamine metabolism. *Oncogene* **21**(54): 8293-8301.
- Caruso S, O'Brien DR, Cleary SP, Roberts LR and Zucman-Rossi J (2020) Genetics of HCC: Novel approaches to explore molecular diversity. *Hepatology*.
- Chandra D, Choy G, Deng X, Bhatia B, Daniel P and Tang DG (2004) Association of active caspase 8 with the mitochondrial membrane during apoptosis: potential roles in cleaving BAP31 and caspase 3 and mediating mitochondrion-endoplasmic reticulum cross talk in etoposide-induced cell death. *Mol Cell Biol* **24**(15): 6592-6607.
- Das S, Nair RS, Mishra R, Sondarva G, Viswakarma N, Abdelkarim H, Gaponenko V, Rana B and Rana A (2019) Mixed lineage kinase 3 promotes breast tumorigenesis via phosphorylation and activation of p21-activated kinase 1. *Oncogene* **38**(19): 3569-3584.

- De A, Jacobson BA, Peterson MS, Jay-Dixon J, Kratzke MG, Sadiq AA, Patel MR and Kratzke RA (2018) 4EGI-1 represses cap-dependent translation and regulates genome-wide translation in malignant pleural mesothelioma. *Invest New Drugs* **36**(2): 217-229.
- de La Coste A, Romagnolo B, Billuart P, Renard CA, Buendia MA, Soubrane O, Fabre M, Chelly J, Beldjord C, Kahn A and Perret C (1998) Somatic mutations of the beta-catenin gene are frequent in mouse and human hepatocellular carcinomas. *Proc Natl Acad Sci U S A* **95**(15): 8847-8851.
- Eom KS, Hong JM, Youn MJ, So HS, Park R, Kim JM and Kim TY (2008) Berberine induces G1 arrest and apoptosis in human glioblastoma T98G cells through mitochondrial/caspases pathway. *Biol Pharm Bull* **31**(4): 558-562.
- Gonsalves FC, Klein K, Carson BB, Katz S, Ekas LA, Evans S, Nagourney R, Cardozo T, Brown AM and DasGupta R (2011) An RNAi-based chemical genetic screen identifies three small-molecule inhibitors of the Wnt/wingless signaling pathway. *Proc Natl Acad Sci U S A* **108**(15): 5954-5963.
- Haghighat A, Mader S, Pause A and Sonenberg N (1995) Repression of cap-dependent translation by 4E-binding protein 1: competition with p220 for binding to eukaryotic initiation factor-4E. *EMBO J* **14**(22): 5701-5709.
- Hawley SA, Ross FA, Chevtzoff C, Green KA, Evans A, Fogarty S, Towler MC, Brown LJ, Ogunbayo OA, Evans AM and Hardie DG (2010) Use of cells expressing gamma subunit variants to identify diverse mechanisms of AMPK activation. *Cell Metab* **11**(6): 554-565.
- Huang Y, Wang K, Gu C, Yu G, Zhao D, Mai W, Zhong Y, Liu S, Nie Y and Yang H (2018) Berberine, a natural plant alkaloid, synergistically sensitizes human liver cancer cells to sorafenib. *Oncol Rep* **40**(3): 1525-1532.

- Huber O, Korn R, McLaughlin J, Ohsugi M, Herrmann BG and Kemler R (1996) Nuclear localization of beta-catenin by interaction with transcription factor LEF-1. *Mech Dev* **59**(1): 3-10.
- Karni R, Gus Y, Dor Y, Meyuhas O and Levitzki A (2005) Active Src elevates the expression of beta-catenin by enhancement of cap-dependent translation. *Mol Cell Biol* **25**(12): 5031-5039.
- Ke R, Vishnoi K, Viswakarma N, Santha S, Das S, Rana A and Rana B (2018) Involvement of AMP-activated protein kinase and Death Receptor 5 in TRAIL-Berberine-induced apoptosis of cancer cells. *Sci Rep* **8**(1): 5521.
- Kim HS, Kim MJ, Kim EJ, Yang Y, Lee MS and Lim JS (2012) Berberine-induced AMPK activation inhibits the metastatic potential of melanoma cells via reduction of ERK activity and COX-2 protein expression. *Biochem Pharmacol* **83**(3): 385-394.
- Kim S, Oh SJ, Lee J, Han J, Jeon M, Jung T, Lee SK, Bae SY, Kim J, Gil WH, Kim SW, Lee JE and Nam SJ (2013) Berberine suppresses TPA-induced fibronectin expression through the inhibition of VEGF secretion in breast cancer cells. *Cell Physiol Biochem* **32**(5): 1541-1550.
- Kong W, Wei J, Abidi P, Lin M, Inaba S, Li C, Wang Y, Wang Z, Si S, Pan H, Wang S, Wu J, Wang Y, Li Z, Liu J and Jiang JD (2004) Berberine is a novel cholesterol-lowering drug working through a unique mechanism distinct from statins. *Nat Med* **10**(12): 1344-1351.
- Korinek V, Barker N, Morin PJ, van Wichen D, de Weger R, Kinzler KW, Vogelstein B and Clevers H (1997) Constitutive transcriptional activation by a beta-catenin-Tcf complex in APC<sup>-/-</sup> colon carcinoma. *Science* **275**(5307): 1784-1787.

- Kotliarova S, Pastorino S, Kovell LC, Kotliarov Y, Song H, Zhang W, Bailey R, Maric D, Zenklusen JC, Lee J and Fine HA (2008) Glycogen synthase kinase-3 inhibition induces glioma cell death through c-MYC, nuclear factor-kappaB, and glucose regulation. *Cancer Res* **68**(16): 6643-6651.
- Krishan S, Richardson DR and Sahni S (2015) Adenosine monophosphate-activated kinase and its key role in catabolism: structure, regulation, biological activity, and pharmacological activation. *Mol Pharmacol* **87**(3): 363-377.
- Laderoute KR, Calaoagan JM, Chao WR, Dinh D, Denko N, Duellman S, Kalra J, Liu X, Papandreou I, Sambucetti L and Boros LG (2014) 5'-AMP-activated protein kinase (AMPK) supports the growth of aggressive experimental human breast cancer tumors. *J Biol Chem* **289**(33): 22850-22864.
- Lee YS, Kim WS, Kim KH, Yoon MJ, Cho HJ, Shen Y, Ye JM, Lee CH, Oh WK, Kim CT, Hohnen-Behrens C, Gosby A, Kraegen EW, James DE and Kim JB (2006) Berberine, a natural plant product, activates AMP-activated protein kinase with beneficial metabolic effects in diabetic and insulin-resistant states. *Diabetes* **55**(8): 2256-2264.
- Li W, Hua B, Saud SM, Lin H, Hou W, Matter MS, Jia L, Colburn NH and Young MR (2015) Berberine regulates AMP-activated protein kinase signaling pathways and inhibits colon tumorigenesis in mice. *Mol Carcinog* **54**(10): 1096-1109.
- Lim S, Saw TY, Zhang M, Janes MR, Nacro K, Hill J, Lim AQ, Chang CT, Fruman DA, Rizzieri DA, Tan SY, Fan H, Chuah CT and Ong ST (2013) Targeting of the MNK-eIF4E axis in blast crisis chronic myeloid leukemia inhibits leukemia stem cell function. *Proc Natl Acad Sci U S A* **110**(25): E2298-2307.

- Lin H, Ying Y, Wang YY, Wang G, Jiang SS, Huang D, Luo L, Chen YG, Gerstenfeld LC and Luo Z (2017) AMPK downregulates ALK2 via increasing the interaction between Smurf1 and Smad6, leading to inhibition of osteogenic differentiation. *Biochim Biophys Acta Mol Cell Res* **1864**(12): 2369-2377.
- Llovet JM and Bruix J (2008) Molecular targeted therapies in hepatocellular carcinoma. *Hepatology* **48**(4): 1312-1327.
- Llovet JM, Ricci S, Mazzaferro V, Hilgard P, Gane E, Blanc JF, de Oliveira AC, Santoro A, Raoul JL, Forner A, Schwartz M, Porta C, Zeuzem S, Bolondi L, Greten TF, Galle PR, Seitz JF, Borbath I, Haussinger D, Giannaris T, Shan M, Moscovici M, Voliotis D and Bruix J (2008) Sorafenib in advanced hepatocellular carcinoma. *N Engl J Med* **359**(4): 378-390.
- Ma XM and Blenis J (2009) Molecular mechanisms of mTOR-mediated translational control. *Nat Rev Mol Cell Biol* **10**(5): 307-318.
- Mishra P, Paramasivam SK, Thylur RP, Rana A and Rana B (2010) Peroxisome proliferator-activated receptor gamma ligand-mediated apoptosis of hepatocellular carcinoma cells depends upon modulation of PI3Kinase pathway independent of Akt. *Journal of molecular signaling* **5**: 20.
- Miyoshi Y, Iwao K, Nagasawa Y, Aihara T, Sasaki Y, Imaoka S, Murata M, Shimano T and Nakamura Y (1998) Activation of the beta-catenin gene in primary hepatocellular carcinomas by somatic alterations involving exon 3. *Cancer Res* **58**(12): 2524-2527.
- Moerke NJ, Aktas H, Chen H, Cantel S, Reibarkh MY, Fahmy A, Gross JD, Degterev A, Yuan J, Chorev M, Halperin JA and Wagner G (2007) Small-molecule inhibition of the



- interaction between the translation initiation factors eIF4E and eIF4G. *Cell* **128**(2): 257-267.
- Molenaar M, van de Wetering M, Oosterwegel M, Peterson-Maduro J, Godsave S, Korinek V, Roose J, Destree O and Clevers H (1996) XTcf-3 transcription factor mediates beta-catenin-induced axis formation in *Xenopus* embryos. *Cell* **86**(3): 391-399.
- Morin PJ, Sparks AB, Korinek V, Barker N, Clevers H, Vogelstein B and Kinzler KW (1997) Activation of beta-catenin-Tcf signaling in colon cancer by mutations in beta-catenin or APC. *Science* **275**(5307): 1787-1790.
- Morin PJ, Vogelstein B and Kinzler KW (1996) Apoptosis and APC in colorectal tumorigenesis. *Proc Natl Acad Sci U S A* **93**(15): 7950-7954.
- Nhieu JT, Renard CA, Wei Y, Cherqui D, Zafrani ES and Buendia MA (1999) Nuclear accumulation of mutated beta-catenin in hepatocellular carcinoma is associated with increased cell proliferation. *Am J Pathol* **155**(3): 703-710.
- Park JJ, Seo SM, Kim EJ, Lee YJ, Ko YG, Ha J and Lee M (2012) Berberine inhibits human colon cancer cell migration via AMP-activated protein kinase-mediated downregulation of integrin beta1 signaling. *Biochem Biophys Res Commun* **426**(4): 461-467.
- Pause A, Belsham GJ, Gingras AC, Donze O, Lin TA, Lawrence JC, Jr. and Sonenberg N (1994) Insulin-dependent stimulation of protein synthesis by phosphorylation of a regulator of 5'-cap function. *Nature* **371**(6500): 762-767.
- Perugorria MJ, Olaizola P, Labiano I, Esparza-Baquer A, Marzioni M, Marin JJG, Bujanda L and Banales JM (2019) Wnt-beta-catenin signalling in liver development, health and disease. *Nat Rev Gastroenterol Hepatol* **16**(2): 121-136.

- Pinyol R, Sia D and Llovet JM (2019) Immune Exclusion-Wnt/CTNNB1 Class Predicts Resistance to Immunotherapies in HCC. *Clin Cancer Res* **25**(7): 2021-2023.
- Porta C and Paglino C (2010) Medical treatment of unresectable hepatocellular carcinoma: Going beyond sorafenib. *World J Hepatol* **2**(3): 103-113.
- Pradeep A, Sharma C, Sathyanarayana P, Albanese C, Fleming JV, Wang TC, Wolfe MM, Baker KM, Pestell RG and Rana B (2004) Gastrin-mediated activation of cyclin D1 transcription involves beta-catenin and CREB pathways in gastric cancer cells. *Oncogene* **23**(20): 3689-3699.
- Ruan H, Zhan YY, Hou J, Xu B, Chen B, Tian Y, Wu D, Zhao Y, Zhang Y, Chen X, Mi P, Zhang L, Zhang S, Wang X, Cao H, Zhang W, Wang H, Li H, Su Y, Zhang XK and Hu T (2017) Berberine binds RXRalpha to suppress beta-catenin signaling in colon cancer cells. *Oncogene* **36**(50): 6906-6918.
- Russell JO and Monga SP (2018) Wnt/beta-Catenin Signaling in Liver Development, Homeostasis, and Pathobiology. *Annu Rev Pathol* **13**: 351-378.
- Santha S, Viswakarma N, Das S, Rana A and Rana B (2015) Tumor Necrosis Factor-related Apoptosis-inducing Ligand (TRAIL)-Troglitazone-induced Apoptosis in Prostate Cancer Cells Involve AMP-activated Protein Kinase. *J Biol Chem* **290**(36): 21865-21875.
- Senthivinayagam S, Mishra P, Paramasivam SK, Yallapragada S, Chatterjee M, Wong L, Rana A and Rana B (2009) Caspase-mediated Cleavage of {beta}-Catenin Precedes Drug-induced Apoptosis in Resistant Cancer Cells. *J Biol Chem* **284**(20): 13577-13588.
- Sharma C, Pradeep A, Wong L, Rana A and Rana B (2004) Peroxisome proliferator-activated receptor gamma activation can regulate beta-catenin levels via a proteasome-mediated

- and adenomatous polyposis coli-independent pathway. *J Biol Chem* **279**(34): 35583-35594.
- Shih IM, Yu J, He TC, Vogelstein B and Kinzler KW (2000) The beta-catenin binding domain of adenomatous polyposis coli is sufficient for tumor suppression. *Cancer Res* **60**(6): 1671-1676.
- Shin S, Wolgamott L, Roux PP and Yoon SO (2014a) Casein kinase 1epsilon promotes cell proliferation by regulating mRNA translation. *Cancer Res* **74**(1): 201-211.
- Shin S, Wolgamott L, Tcherkezian J, Vallabhapurapu S, Yu Y, Roux PP and Yoon SO (2014b) Glycogen synthase kinase-3beta positively regulates protein synthesis and cell proliferation through the regulation of translation initiation factor 4E-binding protein 1. *Oncogene* **33**(13): 1690-1699.
- Stein I, Itin A, Einat P, Skalter R, Grossman Z and Keshet E (1998) Translation of vascular endothelial growth factor mRNA by internal ribosome entry: implications for translation under hypoxia. *Mol Cell Biol* **18**(6): 3112-3119.
- Stoneley M, Chappell SA, Jopling CL, Dickens M, MacFarlane M and Willis AE (2000) c-Myc protein synthesis is initiated from the internal ribosome entry segment during apoptosis. *Mol Cell Biol* **20**(4): 1162-1169.
- Sureau C, Moriarty AM, Thornton GB and Lanford RE (1992) Production of infectious hepatitis delta virus in vitro and neutralization with antibodies directed against hepatitis B virus pre-S antigens. *J Virol* **66**(2): 1241-1245.
- Thylur RP, Senthivinayagam S, Campbell EM, Rangasamy V, Thorenoor N, Sondarva G, Mehrotra S, Mishra P, Zook E, Le PT, Rana A and Rana B (2011) Mixed lineage kinase 3 modulates beta-catenin signaling in cancer cells. *J Biol Chem* **286**(43): 37470-37482.

- Tillhon M, Guaman Ortiz LM, Lombardi P and Scovassi AI (2012) Berberine: new perspectives for old remedies. *Biochem Pharmacol* **84**(10): 1260-1267.
- Torre LA, Bray F, Siegel RL, Ferlay J, Lortet-Tieulent J and Jemal A (2015) Global cancer statistics, 2012. *CA Cancer J Clin* **65**(2): 87-108.
- Tsang CM, Cheung KC, Cheung YC, Man K, Lui VW, Tsao SW and Feng Y (2015) Berberine suppresses Id-1 expression and inhibits the growth and development of lung metastases in hepatocellular carcinoma. *Biochim Biophys Acta* **1852**(3): 541-551.
- Viswakarma N, Nair RS, Sondarva G, Das S, Ibrahim L, Chen Z, Sinha S, Rana B and Rana A (2017) Transcriptional regulation of mixed lineage kinase 3 by estrogen and its implication in ER-positive breast cancer pathogenesis. *Oncotarget* **8**(20): 33172-33184.
- Vlad A, Rohrs S, Klein-Hitpass L and Muller O (2008) The first five years of the Wnt targetome. *Cell Signal* **20**(5): 795-802.
- Wang H, Zhu C, Ying Y, Luo L, Huang D and Luo Z (2018) Metformin and berberine, two versatile drugs in treatment of common metabolic diseases. *Oncotarget* **9**(11): 10135-10146.
- Wang L, Cao H, Lu N, Liu L, Wang B, Hu T, Israel DA, Peek RM, Jr., Polk DB and Yan F (2013) Berberine inhibits proliferation and down-regulates epidermal growth factor receptor through activation of Cbl in colon tumor cells. *PLoS One* **8**(2): e56666.
- Wang N, Feng Y, Zhu M, Tsang CM, Man K, Tong Y and Tsao SW (2010) Berberine induces autophagic cell death and mitochondrial apoptosis in liver cancer cells: the cellular mechanism. *J Cell Biochem* **111**(6): 1426-1436.
- Watanabe K and Dai X (2011) Winning WNT: race to Wnt signaling inhibitors. *Proc Natl Acad Sci U S A* **108**(15): 5929-5930.

- West MJ, Stoneley M and Willis AE (1998) Translational induction of the c-myc oncogene via activation of the FRAP/TOR signalling pathway. *Oncogene* **17**(6): 769-780.
- Wilson W, 3rd and Baldwin AS (2008) Maintenance of constitutive IkappaB kinase activity by glycogen synthase kinase-3alpha/beta in pancreatic cancer. *Cancer Res* **68**(19): 8156-8163.
- Wu K, Yang Q, Mu Y, Zhou L, Liu Y, Zhou Q and He B (2012) Berberine inhibits the proliferation of colon cancer cells by inactivating Wnt/beta-catenin signaling. *Int J Oncol* **41**(1): 292-298.
- Xu L, Zhang Y, Xue X, Liu J, Li ZS, Yang GY, Song Y, Pan Y, Ma Y, Hu S, Wen A, Jia Y, Rodriguez LM, Tull MB, Benante K, Khan SA, Cao Y, Jovanovic B, Richmond E, Umar A, Bergan R and Wu K (2020) A Phase I Trial of Berberine in Chinese with Ulcerative Colitis. *Cancer Prev Res (Phila)* **13**(1): 117-126.
- Yin J, Xing H and Ye J (2008) Efficacy of berberine in patients with type 2 diabetes mellitus. *Metabolism* **57**(5): 712-717.
- Yu R, Zhang ZQ, Wang B, Jiang HX, Cheng L and Shen LM (2014) Berberine-induced apoptotic and autophagic death of HepG2 cells requires AMPK activation. *Cancer cell international* **14**: 49.
- Zhan Y, Dahabieh MS, Rajakumar A, Dobocan MC, M'Boutchou MN, Goncalves C, Lucy SL, Pettersson F, Topisirovic I, van Kempen L, Del Rincon SV and Miller WH, Jr. (2015) The role of eIF4E in response and acquired resistance to vemurafenib in melanoma. *J Invest Dermatol* **135**(5): 1368-1376.
- Zhang H, Wei J, Xue R, Wu JD, Zhao W, Wang ZZ, Wang SK, Zhou ZX, Song DQ, Wang YM, Pan HN, Kong WJ and Jiang JD (2010) Berberine lowers blood glucose in type 2

diabetes mellitus patients through increasing insulin receptor expression. *Metabolism* **59**(2): 285-292.

Zhang J, Cao H, Zhang B, Cao H, Xu X, Ruan H, Yi T, Tan L, Qu R, Song G, Wang B and Hu T (2013) Berberine potently attenuates intestinal polyps growth in ApcMin mice and familial adenomatous polyposis patients through inhibition of Wnt signalling. *J Cell Mol Med* **17**(11): 1484-1493.

Zhao J, Yue W, Zhu MJ, Sreejayan N and Du M (2010) AMP-activated protein kinase (AMPK) cross-talks with canonical Wnt signaling via phosphorylation of beta-catenin at Ser 552. *Biochem Biophys Res Commun* **395**(1): 146-151.

#### **Footnotes:**

This work was supported by the National Institutes of Health National Cancer Institute (grants CA178063 and CA219764 to B.R.), (grants CA176846 and CA216410 to A.R.), and the Veterans Affairs Merit Award (grant BX003296 to B. R.) and (grants BX002703, BX002355 to A. R.).

## Figure Legends:

**Figure 1. Treatment with BBR reduces  $\beta$ -catenin expression in HCC cells.** (A) Huh7 HCC cells were treated with DMSO (-) or BBR-50 $\mu$ M (+) for the indicated time points and then harvested. Equal amounts of protein extracts were analyzed by Western blots against the antibodies indicated. (B) Huh7, (C) Hep3B and (D) HepG2 cells were treated with DMSO (V) or increasing concentrations of BBR (10, 25, 50, 100 $\mu$ M) for 16hrs and analyzed by Western blots.  $\beta$ -catenin-<sub>FL</sub> and  $\beta$ -catenin-<sub>TR</sub> indicate full length (FL) and truncated (TR) forms respectively. The bar graphs represent the ratio of various proteins/controls observed in the western blots. The data represent the mean  $\pm$  S.D. of two to five independent experiments. Statistical analysis was performed using Student's *t*-test and indicated as: ns,  $p > 0.05$ ; \*,  $p \leq 0.05$ ; \*\*,  $p \leq 0.01$ ; \*\*\*  $p \leq 0.001$ , \*\*\*\*  $P \leq 0.0001$ .

**Figure 2. Treatment with BBR antagonizes  $\beta$ -catenin/TCF transcriptional activity and expression of target genes.** (A) HEK-293 and (B) Huh7 cells were transiently transfected with  $\beta$ -catenin/TCF-responsive reporter (pGL3-OT) or the corresponding mutant (pGL3-OF) along with empty vector (EV) or  $\beta$ -catenin-expressing vector and treated with DMSO (-) or indicated concentrations of BBR for 16hrs. Luciferase and  $\beta$ -Gal assays were performed next and the results were expressed as RLU/ $\beta$ -Gal values. Each transfection was performed in triplicate, and each experiment was repeated at least two times. The data represent the mean  $\pm$  S.D of three independent transfections. (C) Equal amounts of protein from Hep3B cells treated with DMSO (V) or BBR for 16hrs were analyzed by Western blots with the antibodies indicated. The bar graphs represent the ratio of various proteins/controls observed in the western blots. The data

represent the mean  $\pm$  S.D. of two independent experiments. Statistical analysis was performed using Student's *t*-test and indicated as: \*,  $p \leq 0.05$ ; \*\*,  $p \leq 0.01$ . **(D)** Total RNA extracted from Huh7 cells treated with DMSO or increasing concentrations of BBR for 16hrs and 24hrs were subjected to qPCR analysis for determining changes in Axin2 gene expression. The experiment was repeated at least three times and data represent the mean  $\pm$  S.D of four independent PCR reactions. Significant differences for (A), (B) and (D) were determined by *t*-test and indicated as: ns,  $p > 0.05$ ; \*,  $p \leq 0.05$ ; \*\*,  $p \leq 0.01$ ; \*\*\*  $p \leq 0.001$ , \*\*\*\*  $P \leq 0.0001$ .

**Figure 3. BBR regulates  $\beta$ -catenin pathway independent of AMPK.** **(A)** Subconfluent populations of Hep3B cells were transiently transfected with control-siRNA, or AMPK $\alpha$ 1-siRNA or  $\alpha$ 2-siRNA alone or in combination followed by treatment with DMSO or BBR for 16hrs. Western blot analyses were performed with the antibodies indicated. **(B)** Hep3B or **(C)** Huh-7 cells stably overexpressing control-shRNA or AMPK  $\alpha$ 1 and  $\alpha$ 2-shRNA were treated with DMSO or BBR for 16hrs and analyzed by western blots. The bar graphs in (A) and (B) represent the ratio of various proteins/controls observed in the western blots. The data represent the mean  $\pm$  S.D. of two independent experiments. Statistical analysis was performed using Student's *t*-test and indicated as: \*,  $p \leq 0.05$ ; \*\*,  $p \leq 0.01$ , \*\*\*  $p \leq 0.001$ . **(D)** Huh7 cells were co-transfected with  $\beta$ -catenin/TCF-responsive reporter (pGL3-OT) and  $\beta$ -catenin-expressing vector along with either control-siRNA, AMPK $\alpha$ 1-siRNA, AMPK $\alpha$ 2-siRNA or AMPK $\alpha$ 1+ $\alpha$ 2-siRNA and treated with DMSO or BBR for 16hrs. Luciferase and  $\beta$ -Gal assays were performed as in Fig 2A and RLU/ $\beta$ -Gal values expressed as % control. Each transfection was performed in triplicate, and each experiment was repeated at least two times. The data represent the mean  $\pm$  S.D of three



independent transfections. Significant differences were determined by *t*-test and indicated as: \*,  $p \leq 0.05$ ; \*\*,  $p \leq 0.01$ ; \*\*\*  $p \leq 0.001$ .

**Figure 4. BBR regulates  $\beta$ -catenin expression at the level of translation.** (A) Total RNA extracted from Huh7 cells as in Fig 2D were subjected to qPCR analysis for determining changes in CTNNB1 ( $\beta$ -catenin) gene expression. The experiment was repeated at least three times and data represent the mean  $\pm$  S.D of 4 independent PCR reactions. Significant differences were determined by *t*-test and indicated as: ns,  $p > 0.05$ ; \*,  $p \leq 0.05$ ; \*\*,  $p \leq 0.01$ . (B) Huh7 cells were treated with either DMSO or Actinomycin D (5 $\mu$ g/ml) or BBR (50 $\mu$ M) or a combination of Actinomycin D and BBR for 24hrs and analyzed by Western blots. (C) Huh7 cells were treated with DMSO (-) or with indicated concentrations of BBR for 24hrs following a pretreatment in the absence or presence of 10 $\mu$ M Lactacystin for 1hr. Equal amounts of lysates were analyzed by western blots. (D) Huh7 cells were treated with DMSO (-) or with indicated concentrations of BBR for 16hrs following a 2hr pretreatment in the absence (-) or presence (+) of 20 $\mu$ M MG132 and analyzed by western blots. (E) Huh7 cells were pretreated with 50 $\mu$ g/ml Cycloheximide (CHX) for 24hrs followed by treatment with DMSO (-) or BBR-50 $\mu$ M (+) in combination with CHX for the indicated periods of time. Lanes 1 and 2 were only treated with DMSO or BBR. The samples were analyzed by western blots with the antibodies indicated. The bar graphs in (C), (D) and (E) represent the ratio of various proteins/controls observed in the western blots. The data represent the mean  $\pm$  S.D. of two to four independent experiments. Statistical analysis was performed using Student's *t*-test and indicated as: \*,  $p \leq 0.05$ ; \*\*,  $p \leq 0.01$ , \*\*\*  $p \leq 0.001$ , \*\*\*\*  $P \leq 0.0001$ .

**Figure 5. BBR inhibits mTOR pathway and cap-dependent translation.** (A) Hep3B and (B) Huh7 cells were treated with DMSO (-) or BBR-50 $\mu$ M (+) for various lengths of time and analyzed by western blots. (C) Huh7 and (D) Hep3B cells were treated with DMSO or with the indicated concentrations of BBR for 16hrs and harvested. Equal amounts of cell extracts were incubated with m<sup>7</sup>GTP agarose beads for 3hrs at 4<sup>0</sup>C. The top panels show m<sup>7</sup>GTP-bound proteins analyzed by western blots and the bottom panels show expression of the corresponding proteins in whole cell lysates.

**Figure 6. BBR-induced reduction of  $\beta$ -catenin involves cap-dependent translation.** (A) Huh7 cells were treated with DMSO (-) or increasing concentrations of BBR for 16hrs following a 2hr pretreatment with or without 4EGI-1 (25 $\mu$ M) and analyzed by western blots. (B) Western blot analysis of extracts from HepG2 cells treated with DMSO (-) or BBR for 24hrs following a 2hr pretreatment with or without 4EGI-1. (C) Stable Huh7 cells overexpressing either a control-shRNA (Huh7-control-shRNA) or eIF4E-BP1- and eIF4E-BP2-shRNA (Huh7-4EBP 1+2-shRNA) were treated with DMSO (-) or BBR (+) for the indicated periods of time. Equal amounts of protein were analyzed by western blots with the antibodies indicated. The bar graphs represent the ratio of various proteins/controls observed in the western blots. The data represent the mean  $\pm$  S.D. of four independent experiments. Statistical analysis was performed using Student's *t*-test and indicated as: \*,  $p \leq 0.05$ ; \*\*\*  $p \leq 0.001$ , \*\*\*\*  $P \leq 0.0001$ . (D) Total RNA extracted from stable Huh7-control-shRNA or Huh7-4EBP 1+2-shRNA cells treated with DMSO (-) or BBR (+) for 48hrs were analyzed by qPCR for Axin2 gene expression. The experiment was repeated twice and data represent the mean  $\pm$  S.D. of two independent PCR reactions. Significant differences were determined by *t*-test and indicated as: ns,  $p > 0.05$ ; \*,  $p \leq$

0.05. **(E)** Huh7-control-shRNA or Huh7-4EBP 1+2-shRNA cells treated with DMSO (-) or BBR (+) for the indicated periods of time were analyzed by western blots.

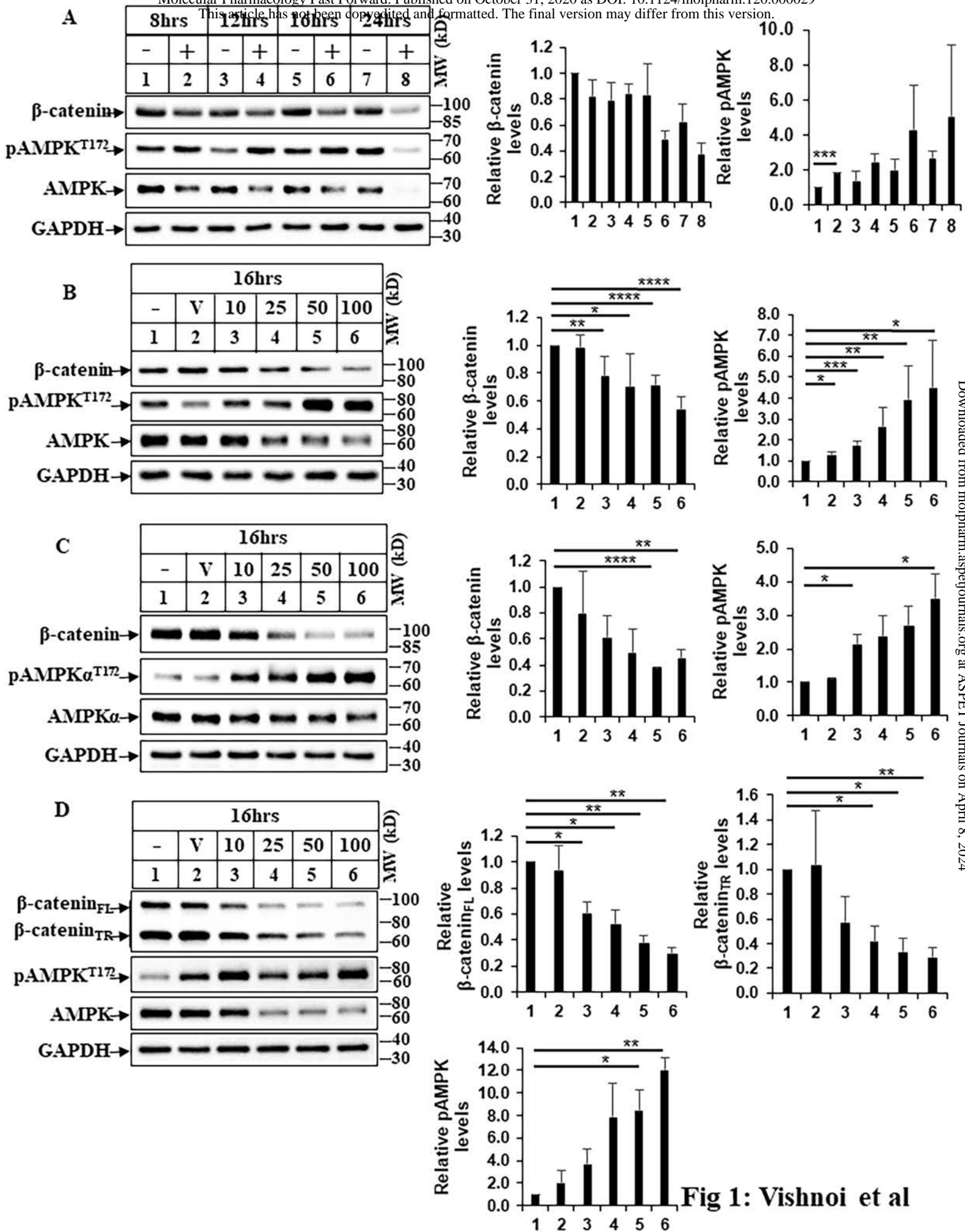
**Figure 7. BBR induces apoptosis via antagonizing cap-dependent translation. (A)**

Representative pictures showing flowcytometric detection of apoptosis assays performed in Huh7-control-shRNA or Huh7-4EBP 1+2-shRNA cells treated with DMSO or BBR (50 $\mu$ M) for 72hrs. Cells were then harvested and apoptosis assays were performed using the FITC Annexin V Apoptosis Detection Kit. The quadrant lines were adjusted to divide the cells in four distinct populations with respect to control. Lower left quadrant represents cells negative for both Annexin V and PI, upper left quadrant represents necrotic cells (only positive for PI), lower right quadrant represents cells in early apoptosis (single positive for Annexin V) and upper right quadrant represents cells in late apoptosis (positive for both Annexin V and PI). **(B)** Huh7-control-shRNA or Huh7-4EBP 1+2-shRNA cells treated as in 7A were analyzed by JC-1 assay to detect changes in mitochondrial membrane potential. The quadrant lines were adjusted to highlight changes in the fluorescent intensity of cell populations with respect to control. Upper right quadrant represents cells containing healthy mitochondria with higher mitochondrial potential emitting a red and a green fluorescence at 590nm and 530nm respectively. Lower right quadrant represents apoptotic cells with reduced mitochondrial membrane potential emitting green fluorescence at 530nm. **(C)** Huh7-control-shRNA or Huh7-4EBP 1+2-shRNA cells treated with DMSO (-) or BBR-50 $\mu$ M (+) for the indicated periods of time were analyzed by western blots with the antibodies indicated.

**Figure 8. BBR induces intrinsic apoptosis via targeting  $\beta$ -catenin.** (A) Representative picture showing flowcytometric analysis of apoptosis assays performed in Huh7-control-shRNA or Huh7-4EBP 1+2-shRNA cells were pretreated with iCRT-14 (10 $\mu$ M) for 24hrs, followed by treatment with iCRT-14 (10 $\mu$ M) alone or in combination with BBR (50 $\mu$ M) for an additional 24hrs. The cells that received DMSO and BBR (50 $\mu$ M) were treated with these for 24hrs. At the end of treatment, cells were harvested and subjected to apoptosis assays and analyzed similarly as described under Fig 7A. (B) Huh7-control-shRNA or Huh7-4EBP 1+2-shRNA cells treated as in 8A were analyzed by JC-1 assay, following procedures described under Fig 7B. (C) The bar graphs represent the ratio of JC-1 Red/JC-1 green. The data represents  $\pm$  S.D. of two independent experiments. Significant differences were determined by *t*-test and indicated as: ns,  $p > 0.05$ ; \*,  $p \leq 0.05$ ; \*\*,  $p \leq 0.01$ . (D) Huh7-control-shRNA or Huh7-4EBP 1+2-shRNA cells were pretreated with iCRT-14 (10 $\mu$ M) for 24hrs, followed by treatment with iCRT-14 (10 $\mu$ M) alone or in combination with BBR (50 $\mu$ M) for an additional 16hrs. The cells that received DMSO and BBR (50 $\mu$ M) were treated with these for 16hrs. At the end of treatment, cells were harvested and fractionated into mitochondrial and cytoplasmic fractions and analyzed by Western blots. COX IV was used a positive control to show the purity of mitochondrial fraction and GAPDH was used as a positive control for cytoplasmic fraction. Cyto C indicates cytochrome c.

**Figure 9: Model illustrating translational regulation of  $\beta$ -catenin by BBR:** (A) In the absence of BBR, an active mTORC1 pathway phosphorylates and inactivates 4EBP1, thus releasing eIF4E from 4EBP1. MNKs then phosphorylate and activate eIF4E. eIF4E interacts with other components of the translational machinery to form eIF4F which is recruited to 5'-mRNA cap to initiate cap-dependent translation of  $\beta$ -catenin. This leads to increased cell

survival. **(B)** BBR inactivates mTORC1 leading to dephosphorylation and activation of 4EBP1 and its interaction with eIF4E. BBR also inhibits MNK-induced eIF4E phosphorylation. This leads to disassembly of eIF4F and repression of  $\beta$ -catenin translation. Repression of  $\beta$ -catenin sensitizes the cells towards increased cell death.



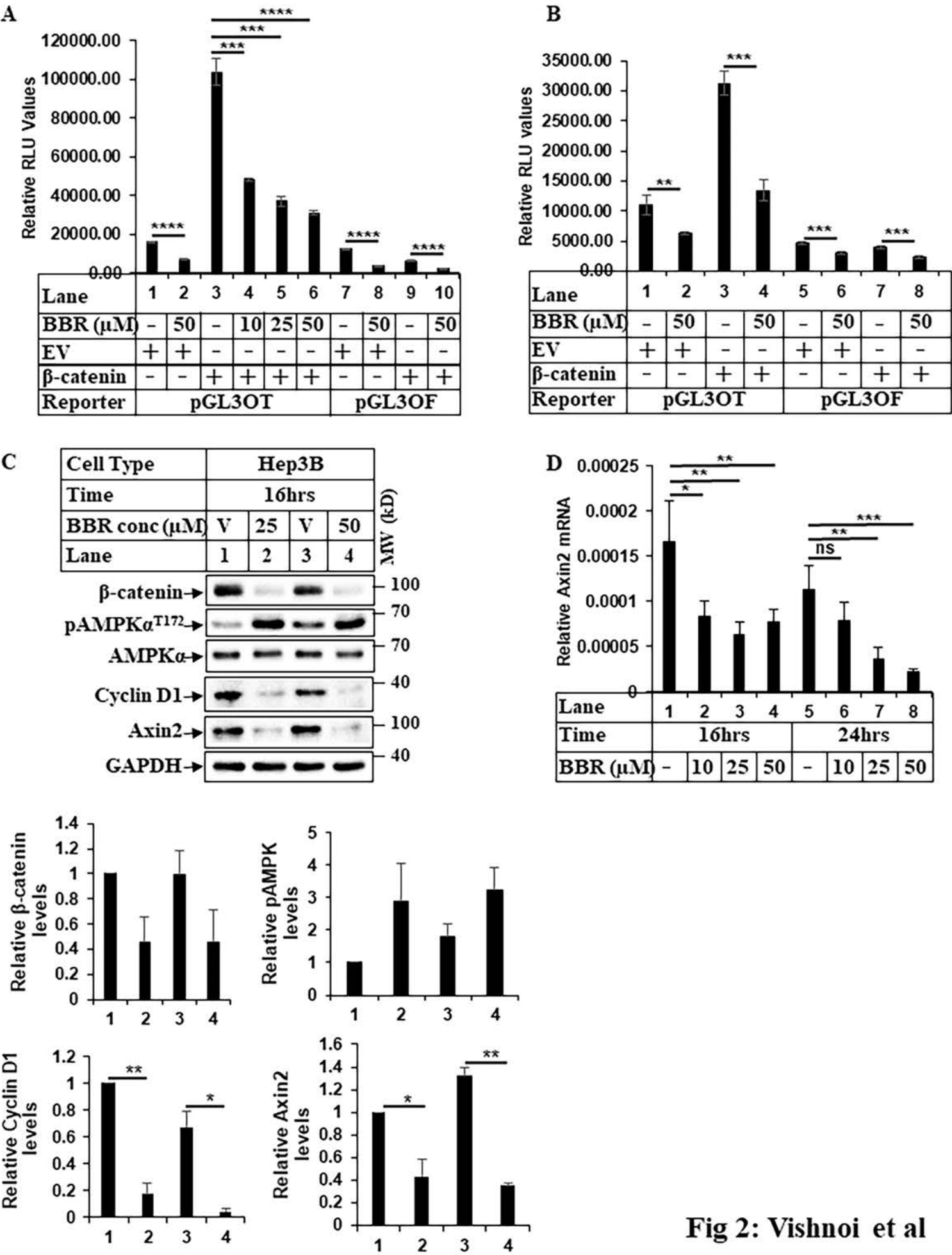


Fig 2: Vishnoi et al

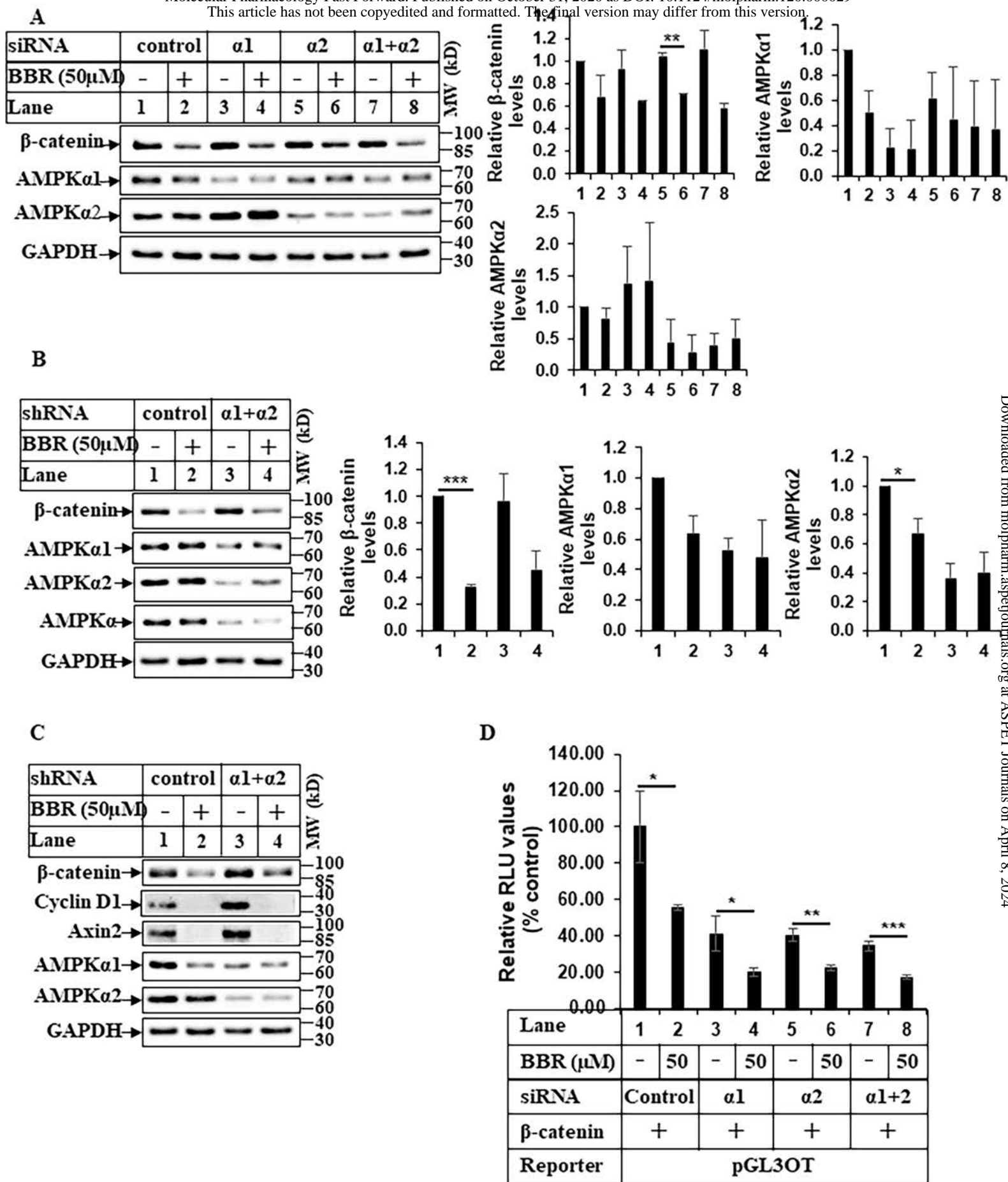


Fig 3: Vishnoi et al



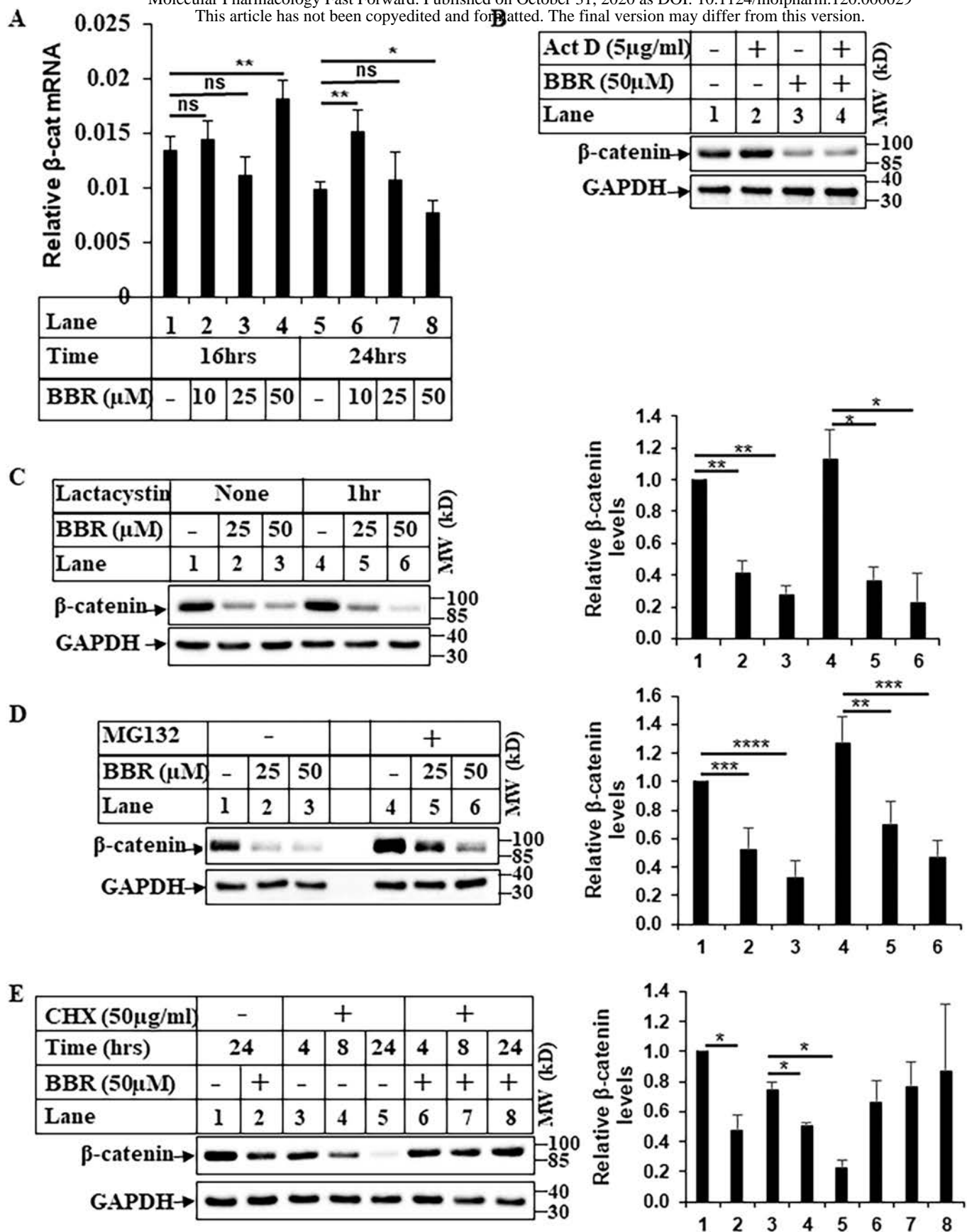
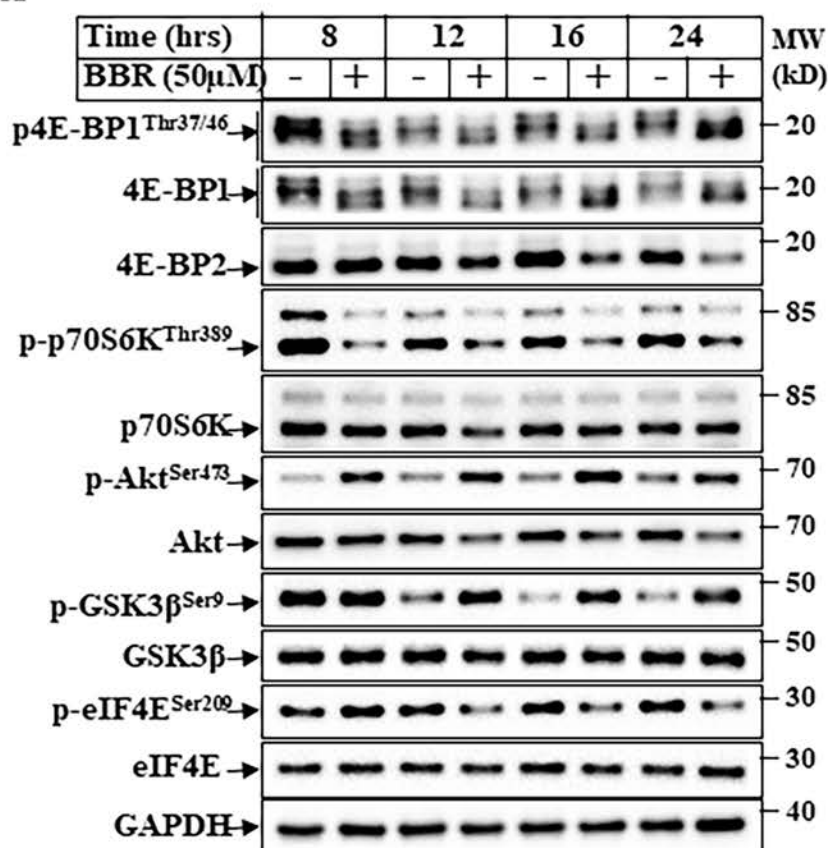
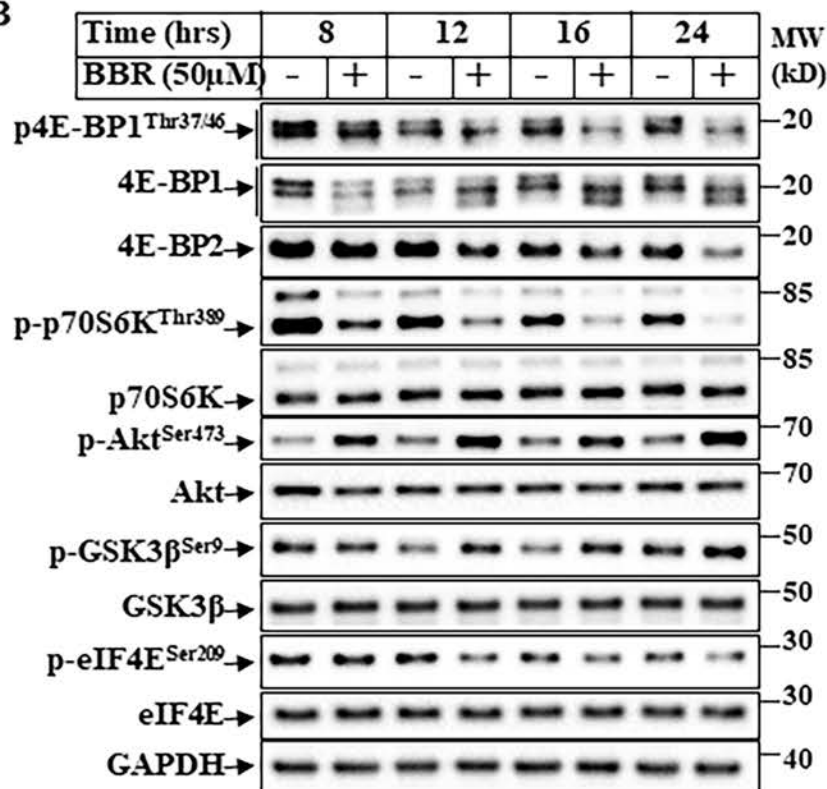


Fig 4: Vishnoi et al

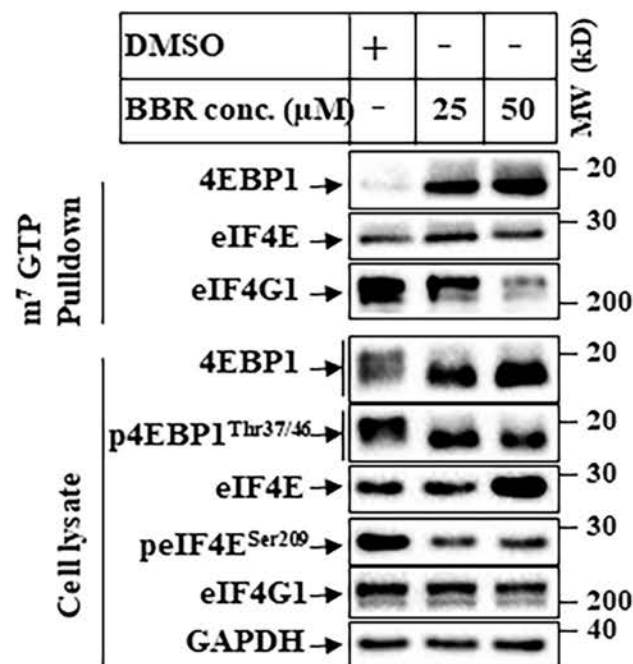
A



B



C



D

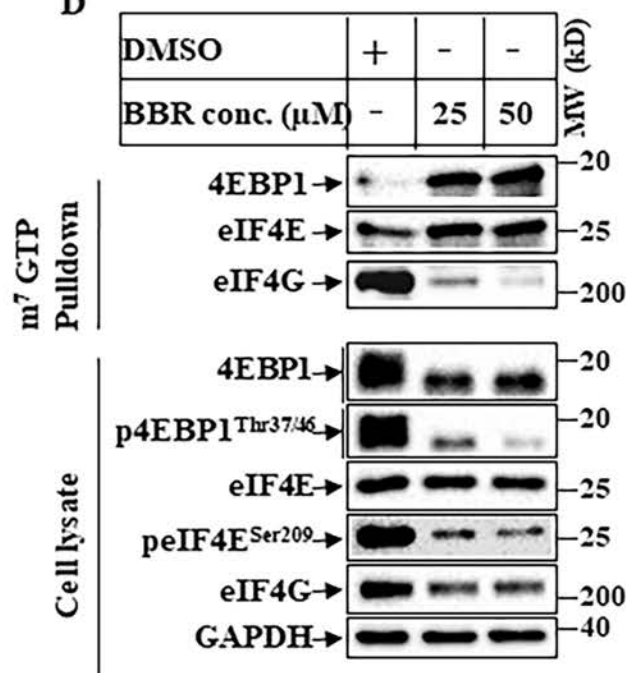


Fig 5: Vishnoi et al

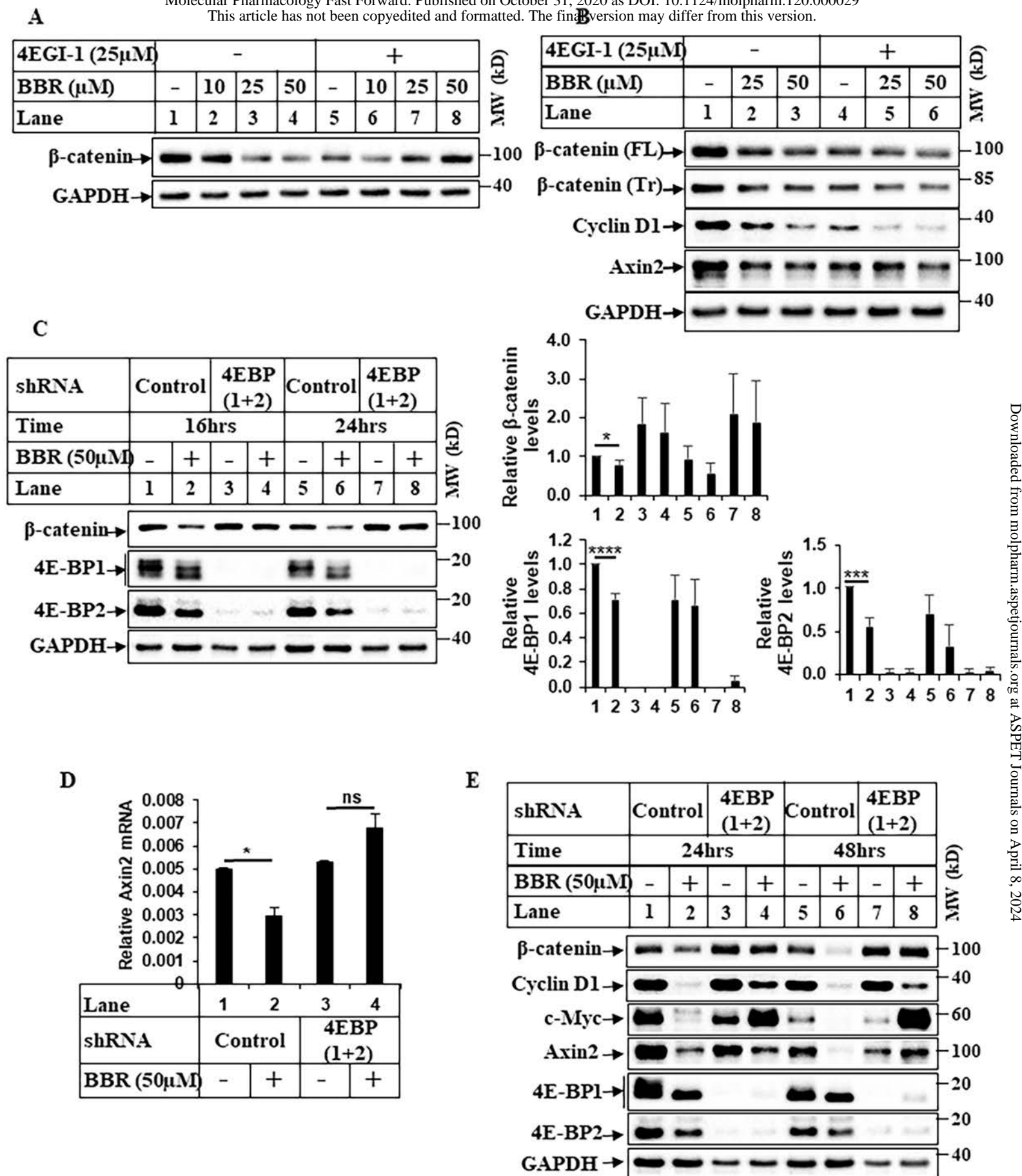
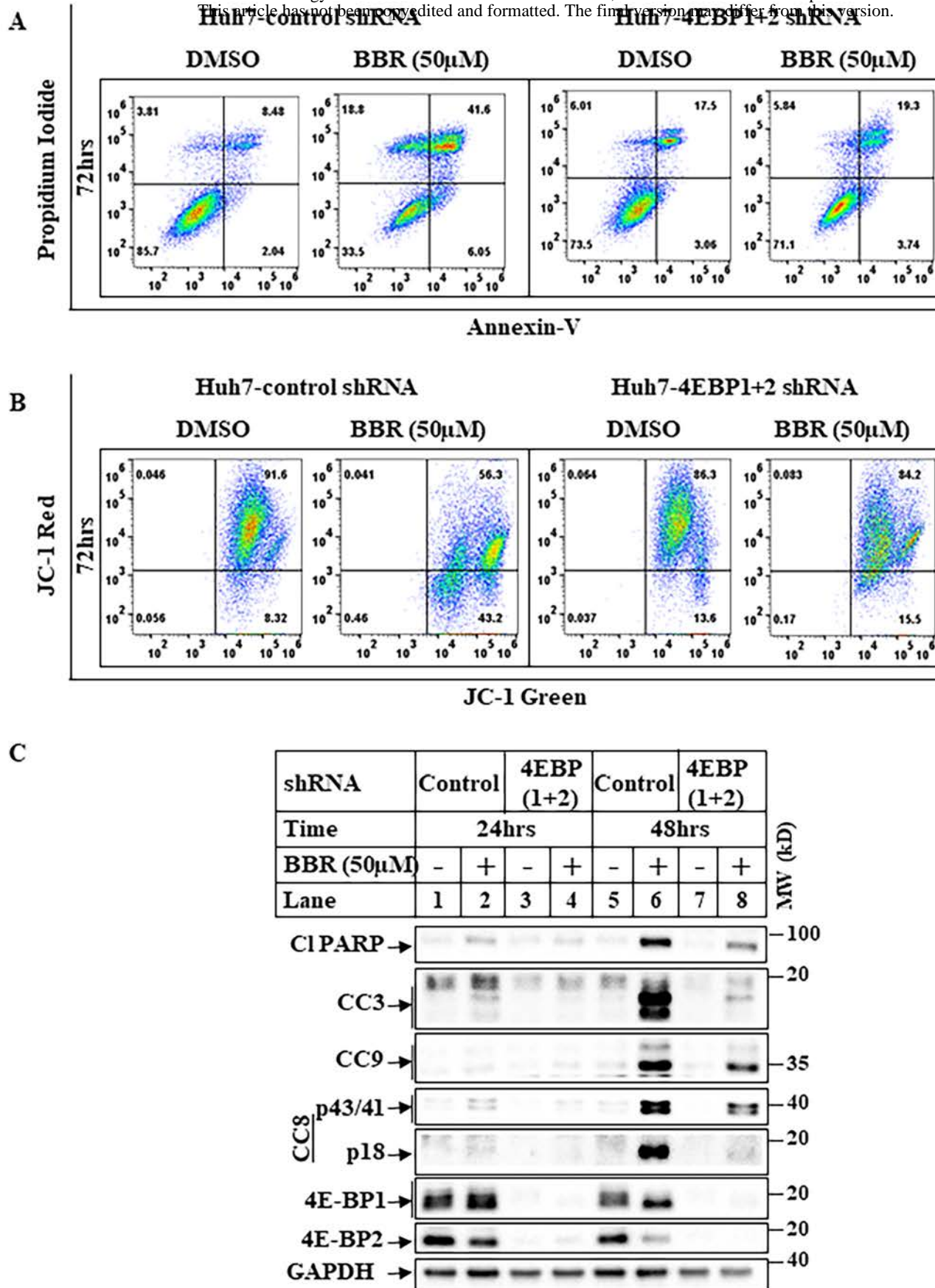


Fig 6: Vishnoi et al



**Fig 7: Vishnoi et al**



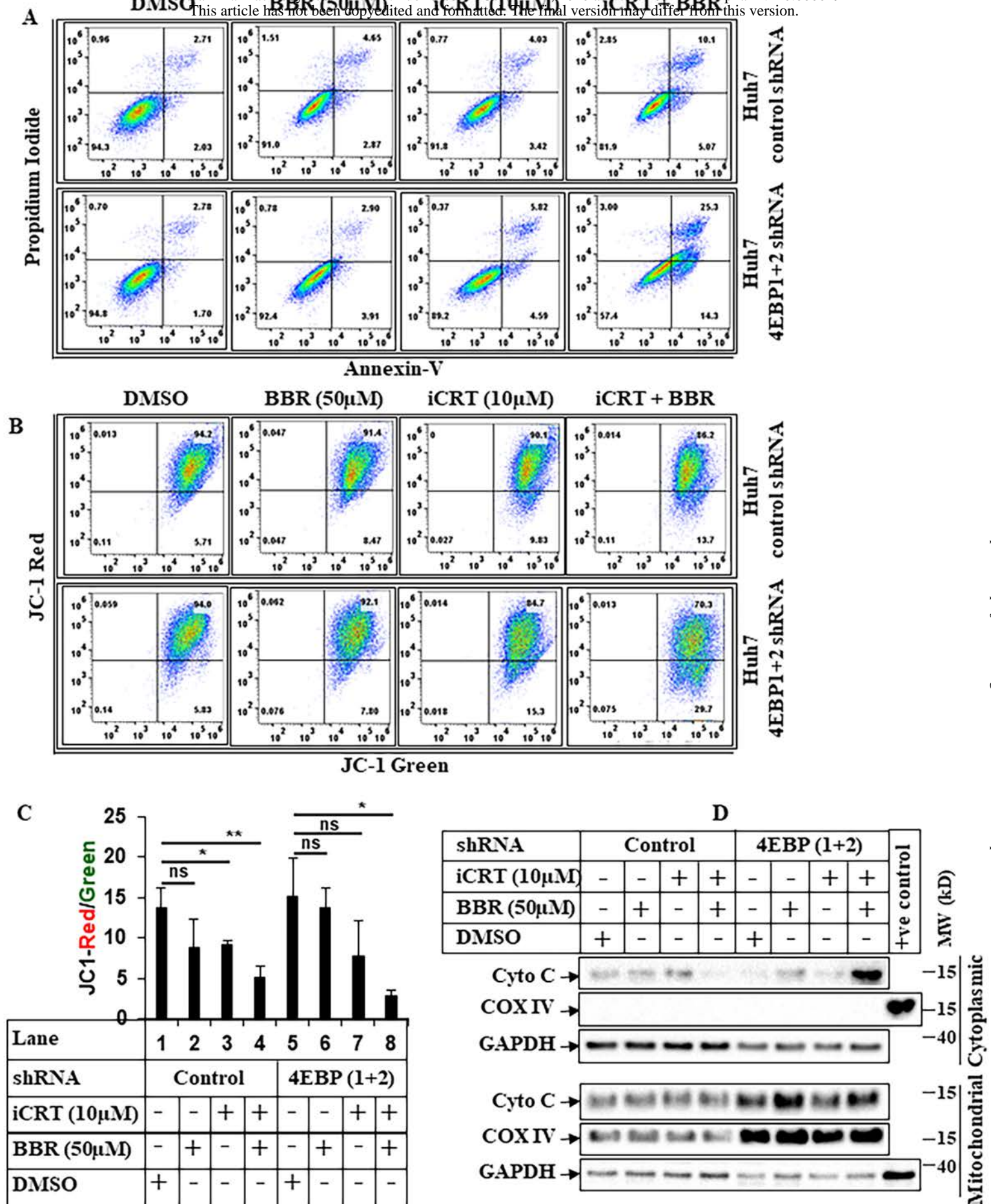


Fig 8: Vishnoi et al

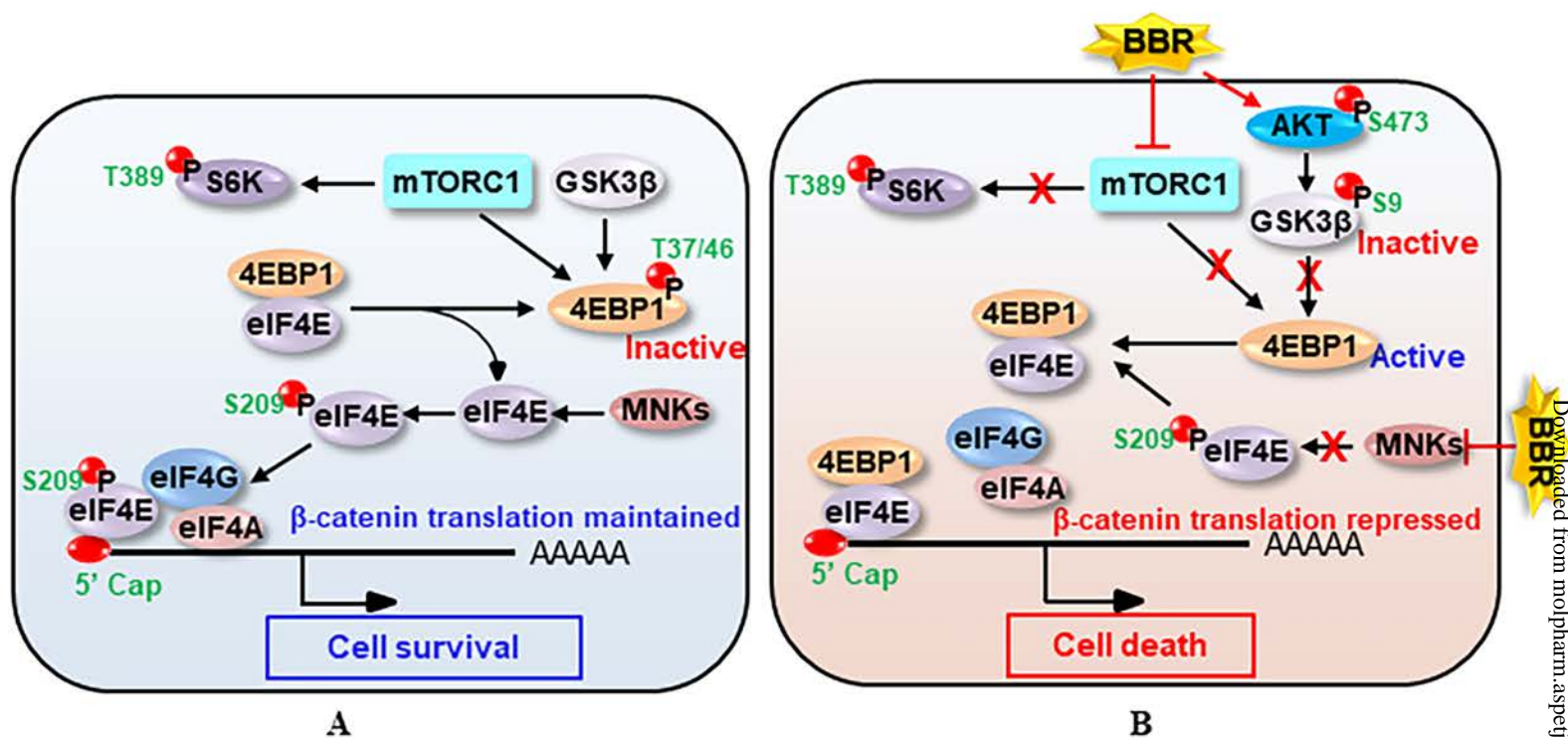


Fig 9: Vishnoi et al

## **Supplementary Information**

### **Berberine represses $\beta$ -catenin translation involving 4E-BPs in hepatocellular carcinoma cells**

Kanchan Vishnoi<sup>1, §</sup>, Rong Ke<sup>1, §</sup>, Karan S Saini<sup>1</sup>, Navin Viswakarma<sup>1</sup>, Rakesh Sathish Nair<sup>1</sup>, Subhasis Das<sup>1, 2</sup>, Zhengjia Chen<sup>3, 4</sup>, Ajay Rana<sup>1, 2, 5</sup>, Basabi Rana<sup>1, 2, 5\*</sup>

<sup>1</sup>Department of Surgery, Division of Surgical Oncology, University of Illinois at Chicago, Chicago, IL-60612, USA

<sup>2</sup>University of Illinois Hospital and Health Sciences System Cancer Center, University of Illinois at Chicago, Chicago, IL-60612, USA

<sup>3</sup>Division of Epidemiology and Biostatistics, School of Public Health, University of Illinois at Chicago, Chicago, IL 60612.

<sup>4</sup>Biostatistics Shared Resource Core, University of Illinois Cancer Institute, Chicago, IL 60612.

<sup>5</sup>Jesse Brown VA Medical Center, Chicago, IL-60612, USA

<sup>§</sup> These authors contributed equally to this work

\*To whom correspondence should be addressed: Clinical Sciences Building, MC 958, Rm. 638, University of Illinois at Chicago, 840 S. Wood Street, Chicago IL 60612, USA. Tel.: 312-996-1078; Fax: 312-996-9365; E-mail: [basrana@uic.edu](mailto:basrana@uic.edu).

**Keywords:** berberine,  $\beta$ -catenin, mTOR, cap-dependent translation, eIF4E-binding protein (4E-BP), hepatocellular carcinoma, WNT signaling, AMP-activated protein kinase

**Running Title:** Berberine represses  $\beta$ -catenin translation

## Supplemental Table 1

### Primers Used for qPCR analysis

Target	Forward	Reverse
$\beta$ -catenin	5'-TCTCCTCAGATGGTGTCTGCT	5'-TGAACCAAGCATTTTCACCAG
Cyclin D1	5'-AGACCTTCGTTGCCCTCTGT	5'-AGTTGTTGGGGCTCCTCAG
c-Myc	5'-AAAGGCCCCCAAGGTAGTTA	5'-GCACAAGAGTTCCGTAGCTG
Axin2	5'-ACTGCCCACACGATAAGGAG	5'-CTGGCTATGTCTTTGCACCA
18S	5'-GGCCCTGTAATTGGAATGAGTC	5'-CCAAGATCCAACCTACGAGCTT



## Supplemental Table 2

### Statistical analysis of data

Figure	Lane	Condition	95% Confidence Interval (CI) of difference with reference	p-value	P value (ANOVA)
Fig. 1A ( $\beta$ -catenin/ GAPDH)	1	DMSO-8hrs	-0.185	0.6837*	0.0006 (By time points) 0.0068 (By treatments) (Two-way ANOVA with replication)
	2	50 $\mu$ M BBR-8hrs	(-0.563, 0.19)		
	3	DMSO-12hrs	0.0476	0.9998*	
	4	50 $\mu$ M BBR-12hrs	(-0.329, 0.425)		
	5	DMSO-16hrs	-0.346	0.0839*	
	6	50 $\mu$ M BBR-16hrs	(-0.723, 0.0306)		
	7	DMSO-24hrs	-0.243	0.3833*	
	8	50 $\mu$ M BBR-24hrs	(-0.620, 0.134)		
Fig. 1A (p-AMPK/ AMPK)	1	DMSO-8hrs	0.7524	0.9993*	0.0787 (By time points) 0.0259 (By treatments) (Two-way ANOVA with replication)
	2	BBR-8hrs	(-4.227, 5.732)		
	3	DMSO-12hrs	1.082	0.9935*	
	4	BBR-12hrs	(-3.898, 6.062)		
	5	DMSO-16hrs	2.329	0.7336*	
	6	BBR-16hrs	(-2.651, 7.308)		
	7	DMSO-24hrs	2.425	0.6958*	
	8	BBR-24hrs	(-2.555, 7.404)		
Fig. 1B ( $\beta$ -catenin/ GAPDH)	1	-	1		<0.0001 (One-way ANOVA)
	2	DMSO	-0.020 (-0.280, 0.240)	0.9999**	
	3	10 $\mu$ M BBR	-0.2303 (-0.4903, 0.0296)	0.1036**	
	4	25 $\mu$ M BBR	-0.305 (-0.564, -0.0447)	0.0151**	
	5	50 $\mu$ M BBR	0.2916 (-0.552, -0.0317)	0.0216**	
	6	100 $\mu$ M BBR	-0.464 (-0.724, -0.204)	0.0001**	
Fig. 1B (p-AMPK/ AMPK)	1	-	1		0.0004 (One-way ANOVA)
	2	DMSO	0.227 (-2.162, 2.617)	0.9997**	
	3	10 $\mu$ M BBR	0.726 (-1.664, 3.116)	0.9322**	
	4	25 $\mu$ M BBR	1.613 (-0.776, 4.003)	0.3266**	
	5	50 $\mu$ M BBR	2.930 (0.5399, 5.319)	0.0102**	
	6	100 $\mu$ M BBR	3.454	0.0020**	

			(1.065, 5.844)		
Fig. 1C ( $\beta$ -catenin/ GAPDH)	1	-	1		0.06829 (One-way ANOVA)
	2	DMSO	-0.2083 (-0.8968, 0.4802)	0.8217**	
	3	10 $\mu$ M BBR	-0.3985 (-1.087, 0.290)	0.3172**	
	4	25 $\mu$ M BBR	-0.5131 (-1.2016, 0.1755)	0.1523**	
	5	50 $\mu$ M BBR	-0.6238 (-1.3123, 0.0647)	0.0748**	
	6	100 $\mu$ M BBR	-0.5569 (-1.2454, 0.1316)	0.1146**	
Fig. 1C (p-AMPK/ AMPK)	1	-	1		0.01442 (One-way ANOVA)
	2	DMSO	-0.1018 (-1.840, 2.044)	0.9999**	
	3	10 $\mu$ M BBR	1.113 (-0.8288, 3.055)	0.3247**	
	4	25 $\mu$ M BBR	1.359 (-0.583, 3.30)	0.1864**	
	5	50 $\mu$ M BBR	1.675 (-0.2672, 3.6166)	0.0905**	
	6	100 $\mu$ M BBR	2.474 (0.5323, 4.416)	0.0168**	
Fig. 1D ( $\beta$ -catenin (FL)/ GAPDH)	1	-	1		0.00286 (One-way ANOVA)
	2	DMSO	-0.0737 (-0.5046, 0.357)	0.9779**	
	3	10 $\mu$ M BBR	-0.399 (-0.83, 0.318)	0.0685**	
	4	25 $\mu$ M BBR	-0.488 (-0.919, -0.057)	0.029**	
	5	50 $\mu$ M BBR	-0.623 (-1.054, -0.192)	0.009**	
	6	100 $\mu$ M BBR	-0.705 (-1.136, -0.274)	0.0048**	
Fig. 1D ( $\beta$ -catenin (TR)/ GAPDH)	1	-	1		0.04057 (One-way ANOVA)
	2	DMSO	0.033 (-0.8162, 0.8826)	1.0**	
	3	10 $\mu$ M BBR	-0.4299 (-1.2793, 0.4195)	0.4282**	
	4	25 $\mu$ M BBR	-0.586 (-1.436, 0.263)	0.1948**	
	5	50 $\mu$ M BBR	-0.666	0.1278**	

			(-1.516, 0.183)		
	6	100μM BBR	-0.711 (-1.56, 0.139)	0.1013**	
Fig. 1D (p-AMPK/ AMPK)	1	-	1		0.0036 (One-way ANOVA)
	2	DMSO	0.984 (-5.709, 7.676)	0.9884**	
	3	10μM BBR	2.617 (-4.076, 9.309)	0.6485**	
	4	25μM BBR	6.854 (0.161, 13.546)	0.0452**	
	5	50μM BBR	7.401 (0.7086, 14.094)	0.0323**	
	6	100μM BBR	11.031 (4.338, 17.723)	0.0046**	
Fig. 2C (β-catenin/ GAPDH)	1	5μl DMSO	-0.5414	0.1442*	<0.0001 (By dose) <0.0001 (By treatments) (Two-way ANOVA with replication)
	2	25μM BBR	(-1.3174, 0.2347)		
	3	10μl DMSO	-0.533	0.1503*	
	4	50μM BBR	(-1.309, 0.243)		
Fig. 2C (Cyclin D1/ GAPDH)	1	5μl DMSO	-0.8283	0.0013*	<0.0001 (By dose) <0.0001 (By treatments) (Two-way ANOVA with replication)
	2	25μM BBR	(-1.129, -0.5278)		
	3	10μl DMSO	-0.6314	0.0036*	
	4	50μM BBR	(-0.932, -0.331)		
Fig. 2C (p-AMPK/ AMPK)	1	5μl DMSO	1.8964	0.1694*	<0.0001 (By dose) <0.0001 (By treatments) (Two-way ANOVA with replication)
	2	25μM BBR	(-0.9967, 4.7896)		
	3	10μl DMSO	1.435	0.316*	
	4	50μM BBR	(-1.458, 4.328)		
Fig. 2C (Axin2/ GAPDH)	1	5μl DMSO	-0.5684	0.0092*	<0.0001 (By dose) <0.0001 (By treatments) (Two-way ANOVA with replication)
	2	25μM BBR	(-0.917, -0.219)		
	3	10μl DMSO	-0.967	0.0012*	
	4	50μM BBR	(-1.316, -0.618)		
Fig. 3A (β-catenin/ GAPDH)	1	Cont si-DMSO	-0.3228	0.2071*	<0.0001 (By treatments) 0.7307 (By siRNAs) (Two-way ANOVA with replication)
	2	Cont si-50μM BBR	(-0.7728, 0.127)		
	3	α1 si-DMSO	-0.285	0.3101*	
	4	α1 si-50μM BBR	(-0.735, 0.165)		
	5	α2 si-DMSO	-0.33	0.1926*	
	6	α2 si-50μM BBR	(-0.779, 0.1204)		
	7	α1&2 si-DMSO	-0.522	0.0227*	
	8	α1&2 si-50μM BBR	(-0.972, -0.0723)		
Fig. 3A (AMPKα1/ GAPDH)	1	Cont si-DMSO	-0.503	0.6363*	0.22 (By treatments) 0.08 (By siRNAs) (Two-way ANOVA with
	2	Cont si-50μM BBR	(-1.609, 0.603)		
	3	α1 si-DMSO	-0.009	1.0*	

	4	$\alpha$ 1 si-50 $\mu$ M BBR	(-1.115, 1.097)		replication)
	5	$\alpha$ 2 si-DMSO	-0.161	0.998*	
	6	$\alpha$ 2 si-50 $\mu$ M BBR	(-1.267, 0.945)		
	7	$\alpha$ 1&2 si-DMSO	-0.0214	1.0*	
	8	$\alpha$ 1&2 si-50 $\mu$ M BBR	(-1.127, 1.085)		
Fig. 3A (AMPK $\alpha$ 2/ GAPDH)	1	Cont si-DMSO	-0.2027	0.99*	0.80 (By treatments) 0.0124 (By siRNAs) (Two-way ANOVA with replication)
	2	Cont si-50 $\mu$ M BBR	(-2.0, 1.594)		
	3	$\alpha$ 1 si-DMSO	0.0298	1.0*	
	4	$\alpha$ 1 si-50 $\mu$ M BBR	(-1.767, 1.827)		
	5	$\alpha$ 2 si-DMSO	-0.135	1.0*	
	6	$\alpha$ 2 si-50 $\mu$ M BBR	(-1.932, 1.66)		
	7	$\alpha$ 1&2 si-DMSO	0.1036	1.0*	
	8	$\alpha$ 1&2 si-50 $\mu$ M BBR	(-1.693, 1.90)		
Fig. 3B ( $\beta$ -catenin/ GAPDH)	1	Cont sh-DMSO	-0.682	0.0179*	0.001 (By treatments) 0.6091 (By siRNAs) (Two-way ANOVA with replication)
	2	Cont sh-50 $\mu$ M BBR	(-1.186, -0.179)		
	3	$\alpha$ 1&2 sh-DMSO	-0.516	0.0464*	
	4	$\alpha$ 1&2 sh-50 $\mu$ M BBR	(-1.02, -0.012)		
Fig. 3B (AMPK $\alpha$ 1/ GAPDH)	1	Cont sh-DMSO	-0.371	0.192*	0.1387 (By treatments) 0.0436 (By siRNAs) (Two-way ANOVA with replication)
	2	Cont sh-50 $\mu$ M BBR	(-0.966, 0.224)		
	3	$\alpha$ 1&2 sh-DMSO	-0.044	0.9891*	
	4	$\alpha$ 1&2 sh-50 $\mu$ M BBR	(-0.639, 0.551)		
Fig. 3B (AMPK $\alpha$ 2/ GAPDH)	1	Cont sh-DMSO	-0.333	0.1025*	0.2239 (By treatments) 0.0078 (By siRNAs) (Two-way ANOVA with replication)
	2	Cont sh-50 $\mu$ M BBR	(-0.754, 0.0885)		
	3	$\alpha$ 1&2 sh-DMSO	0.039	0.9793*	
	4	$\alpha$ 1&2 sh-50 $\mu$ M BBR	(-0.382, 0.460)		
Fig. 4C ( $\beta$ -catenin/ GAPDH)	1	(-)Lac-DMSO	1	Reference	<0.0001 (By treatments) 0.8651 (By -/+Lac) (Two-way ANOVA with replication)
	2	(-)Lac-25 $\mu$ M BBR	-0.5884 (-1.066, -0.111)	0.0197*	
	3	(-)Lac-50 $\mu$ M BBR	-0.7254 (-1.2032, -0.2475)	0.0071*	
	4	(+)Lac-DMSO	1.129 $\pm$ 1.687	Reference	
	5	(+)Lac-25 $\mu$ M BBR	-0.7622 (-1.240, -0.2844)	0.0055*	
	6	(+)Lac-50 $\mu$ M BBR	-0.9033 (-1.381, -0.425)	0.0022*	
Fig. 4D ( $\beta$ -catenin/ GAPDH)	1	(-)MG-DMSO	1	Reference	<0.0001 (By treatments) 0.0022 (By -/+MG) (Two-way ANOVA with replication)
	2	(-)MG-25 $\mu$ M BBR	-0.4823 (-0.7965, -0.1681)	0.0014*	
	3	(-)MG-50 $\mu$ M BBR	-0.6725 (-0.9867, -0.3583)	<0.0001*	
	4	(+)MG-DMSO	1.265 $\pm$ 0.301	Reference	
	5	(+)MG-25 $\mu$ M BBR	-0.5661	0.002*	

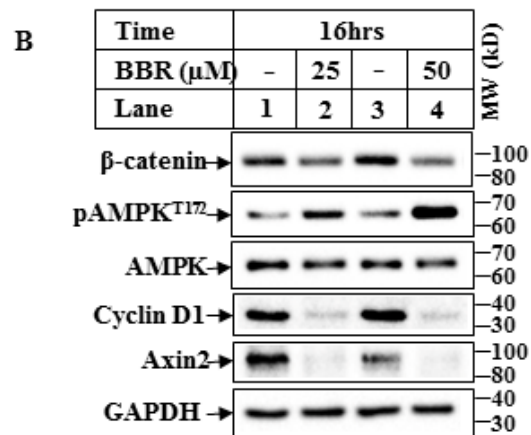
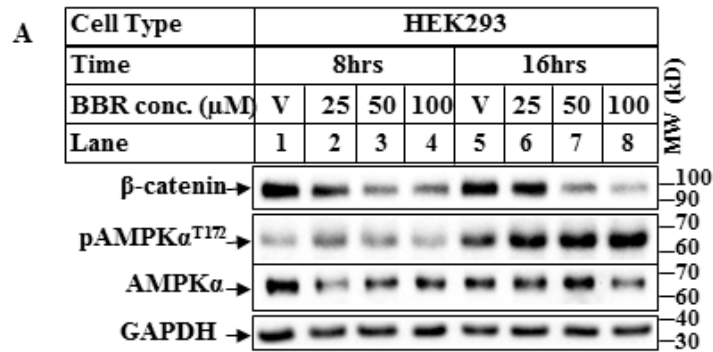
			(-0.8803, -0.2519)		
	6	(+)MG-50μM BBR	-0.7981 (-1.1124, -0.4839)	<0.0001*	
Fig. 4E (β-catenin/ GAPDH)	1	DMSO-24hrs	1	0.1933*	0.5643 (By CHX treatment) 0.645 (By DMSO/BBR) 0.9347 (By Time) (Three-way ANOVA with replication)
	2	50μM BBR-24hrs	-0.529 (-1.252, 0.1942)		
	3	DMSO-CHX-4hrs	0.744 ± 0.469	Reference	
	4	DMSO-CHX-8hrs	-0.2366 (-0.9599, 0.4867)	0.8784*	
	5	DMSO-CHX-24hrs	-0.5197 (-1.243, 0.2036)	0.2061*	
	6	50μM BBR-CHX-4hrs	0.666 ± 1.293	Reference	
	7	50μM BBR-CHX-8hrs	0.0962 (-0.6272, 0.8195)	0.999*	
	8	50μM BBR-CHX- 24hrs	0.2063 (-0.517, 0.930)	0.9322*	
Fig. 6C (β-catenin/ GAPDH)	1	Cont sh-DMSO-16hrs	-0.2476 (-1.339, 0.8436)	0.9051*	0.3901 (By treatments) 0.0055 (By shRNA) (Two-way ANOVA with replication)
	2	Cont sh-50μM BBR- 16hrs			
	3	4EBP1&2 sh-DMSO- 16hrs	-0.1966 (-1.2878, 0.8945)	0.9488*	
	4	4EBP1&2 sh-50μM BBR-16hrs			
	5	Cont sh-DMSO-24hrs	-0.375 (-2.044, 1.294)	0.9075*	0.4622 (By treatments) 0.006 (By siRNAs) (Two-way ANOVA with replication)
	6	Cont sh-50μM BBR- 24hrs			
	7	4EBP1&2 sh-DMSO- 24hrs	-0.205 (-1.874, 1.464)	0.9826*	
	8	4EBP1&2 sh-50μM BBR-24hrs			
Fig. 6C (4EBP1/ GAPDH)	1	Cont sh-DMSO-16hrs	-0.295 (-0.354, -0.237)	<0.0001*	0.0045 (By treatments) <0.0001 (By shRNAs) (Two-way ANOVA with replication)
	2	Cont sh-50μM BBR- 16hrs			
	3	4EBP1&2 sh-DMSO- 16hrs	0	1.0*	
	4	4EBP1&2 sh-50μM BBR-16hrs			
	5	Cont sh-DMSO-24hrs	-0.0455 (-0.3709, 0.2798)	0.9747*	0.9601 (By treatments) <0.0001 (By shRNAs) (Two-way ANOVA with replication)
	6	Cont sh-50μM BBR- 24hrs			
	7	4EBP1&2 sh-DMSO- 24hrs	0.0379 (-0.2875, 0.3632)	0.9851*	
	8	4EBP1&2 sh-50μM BBR-24hrs			

Fig. 6C (4EBP2/ GAPDH)	1	Cont sh-DMSO-16hrs	-0.4546 (-0.5937, -0.3155)	<0.0001*	0.0069 (By treatments) <0.0001 (By shRNAs) (Two-way ANOVA with replication)
	2	Cont sh-50μM BBR-16hrs			
	3	4EBP1&2 sh-DMSO-16hrs	0.00132 (-0.1378, 0.1405)	1.00*	
	4	4EBP1&2 sh-50μM BBR-16hrs			
	5	Cont sh-DMSO-24hrs	-0.3937 (-0.7614, -0.026)	0.0348*	0.0862 (By treatments) 0.0004 (By shRNAs) (Two-way ANOVA with replication)
	6	Cont sh-50μM BBR-24hrs			
	7	4EBP1&2 sh-DMSO-24hrs	0.0165 (-0.3512, 0.3843)	0.9991*	
	8	4EBP1&2 sh-50μM BBR-24hrs			

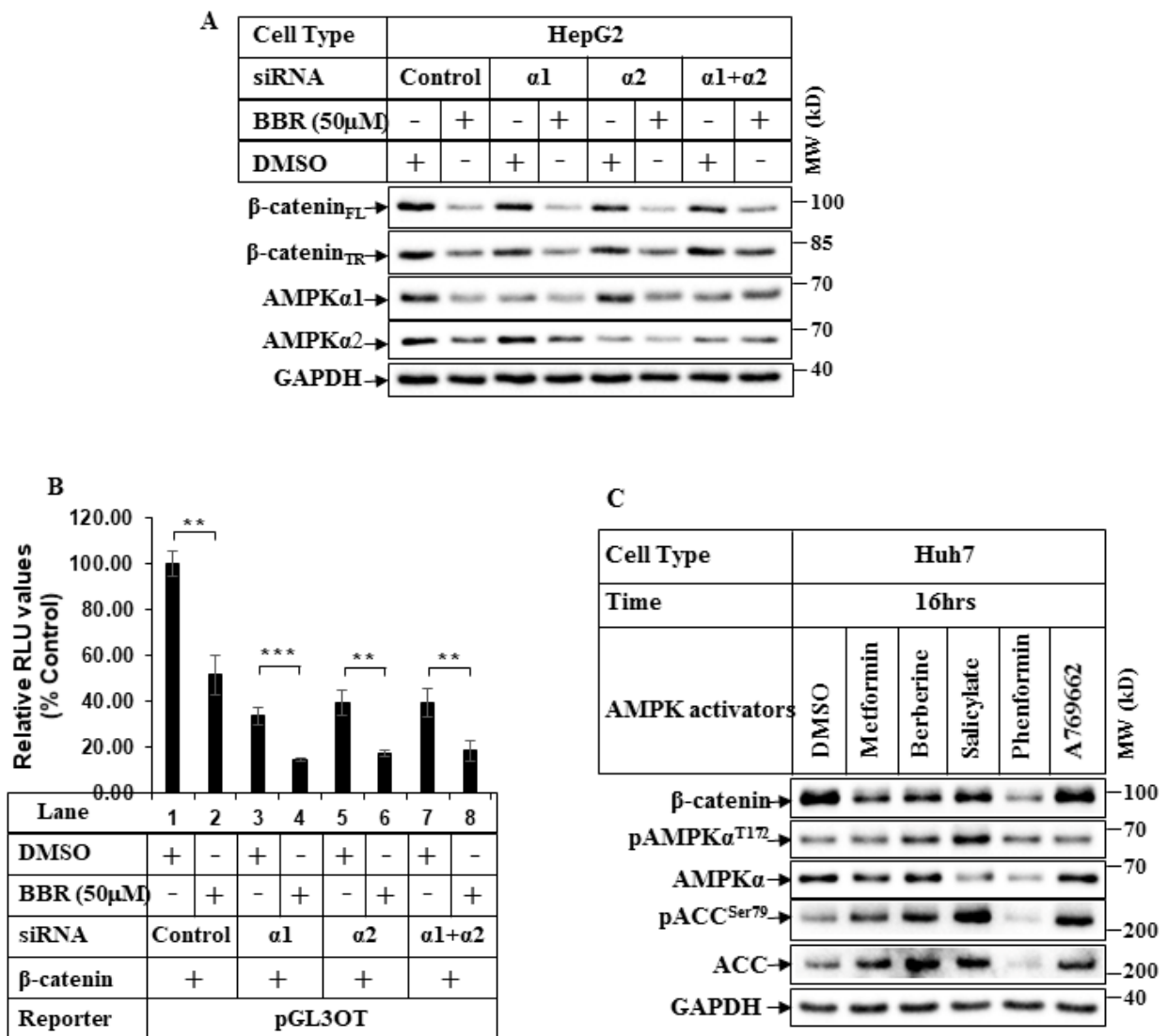
\*: p-value from Tukey's test

\*\*: p-value from Dunnett's test.

## Supplementary Data:

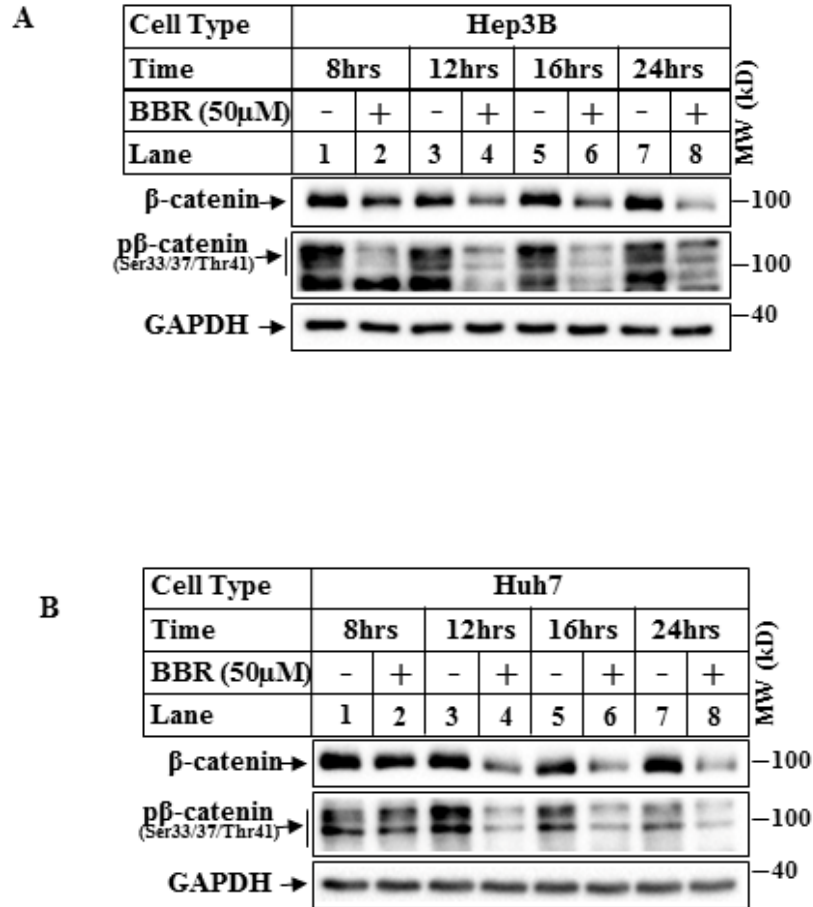


**Supplemental Figure 1: Effect of increasing concentrations of BBR on  $\beta$ -catenin pathway:** (A) HEK293 cells were treated with vehicle (V) or indicated concentrations of BBR for 8hrs or 16hrs and analyzed by Western blots. (B) Huh7 cells treated with vehicle (-) or BBR for 16hrs were analyzed by western blots with the antibodies indicated.

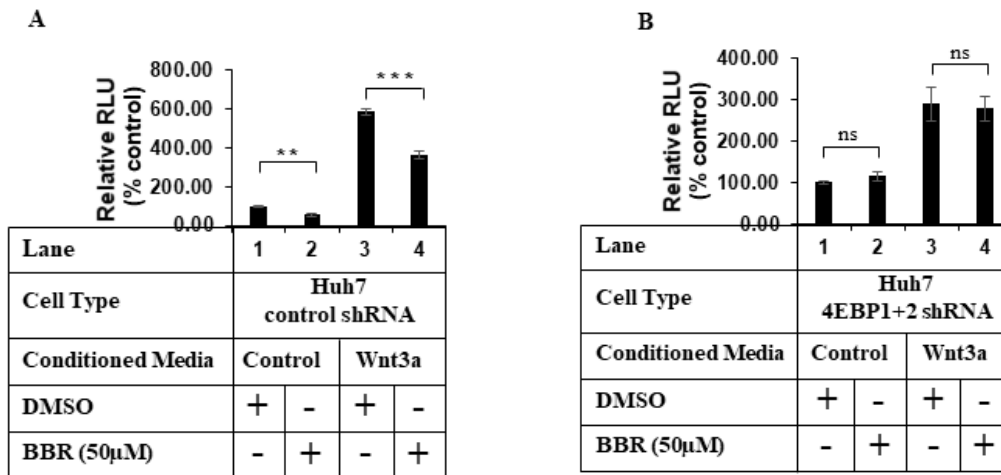


**Supplemental Figure 2: BBR regulates  $\beta$ -catenin pathway independent of AMPK:** (A) HepG2 cells were transiently transfected with control-siRNA, or AMPK $\alpha 1$ -siRNA or  $\alpha 2$ -siRNA alone or in combination followed by treatment with DMSO or BBR for 16hrs. Western blot analyses were performed with the antibodies indicated. (B) HEK-293 cells were co-transfected with  $\beta$ -catenin/TCF-responsive reporter (pGL3-OT) and  $\beta$ -catenin-expressing vector along with the indicated siRNAs and treated with DMSO or BBR for 16hrs. Luciferase and  $\beta$ -Gal assays were performed as in Fig 3D. The data represent the mean  $\pm$  S.D. of three independent transfections. Significant differences were determined by *t*-test and indicated as: \*\*,  $p \leq 0.01$ ; \*\*\*  $p \leq 0.001$ . (C) Huh7 cells were treated with either DMSO, Metformin (10mM), BBR (25 $\mu$ M), Salicylate (25 $\mu$ M), Phenformin (1mM) or A769662 (10 $\mu$ M) for 16hrs and analyzed by western blots.

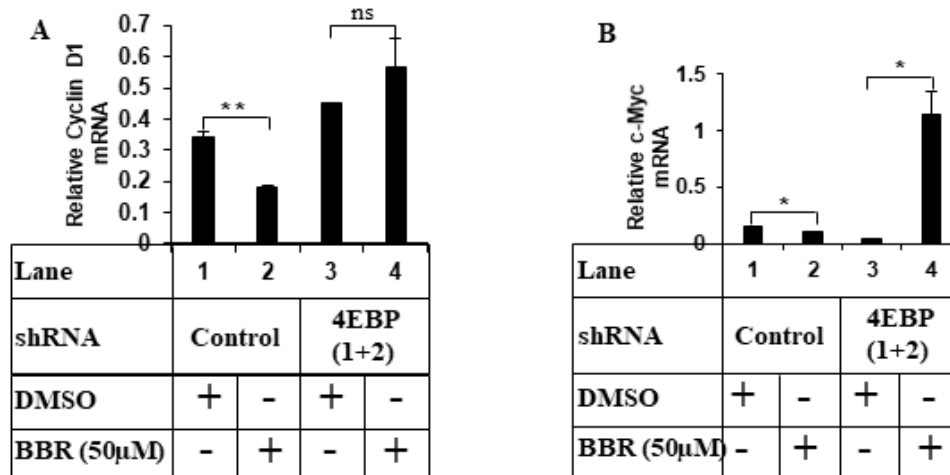




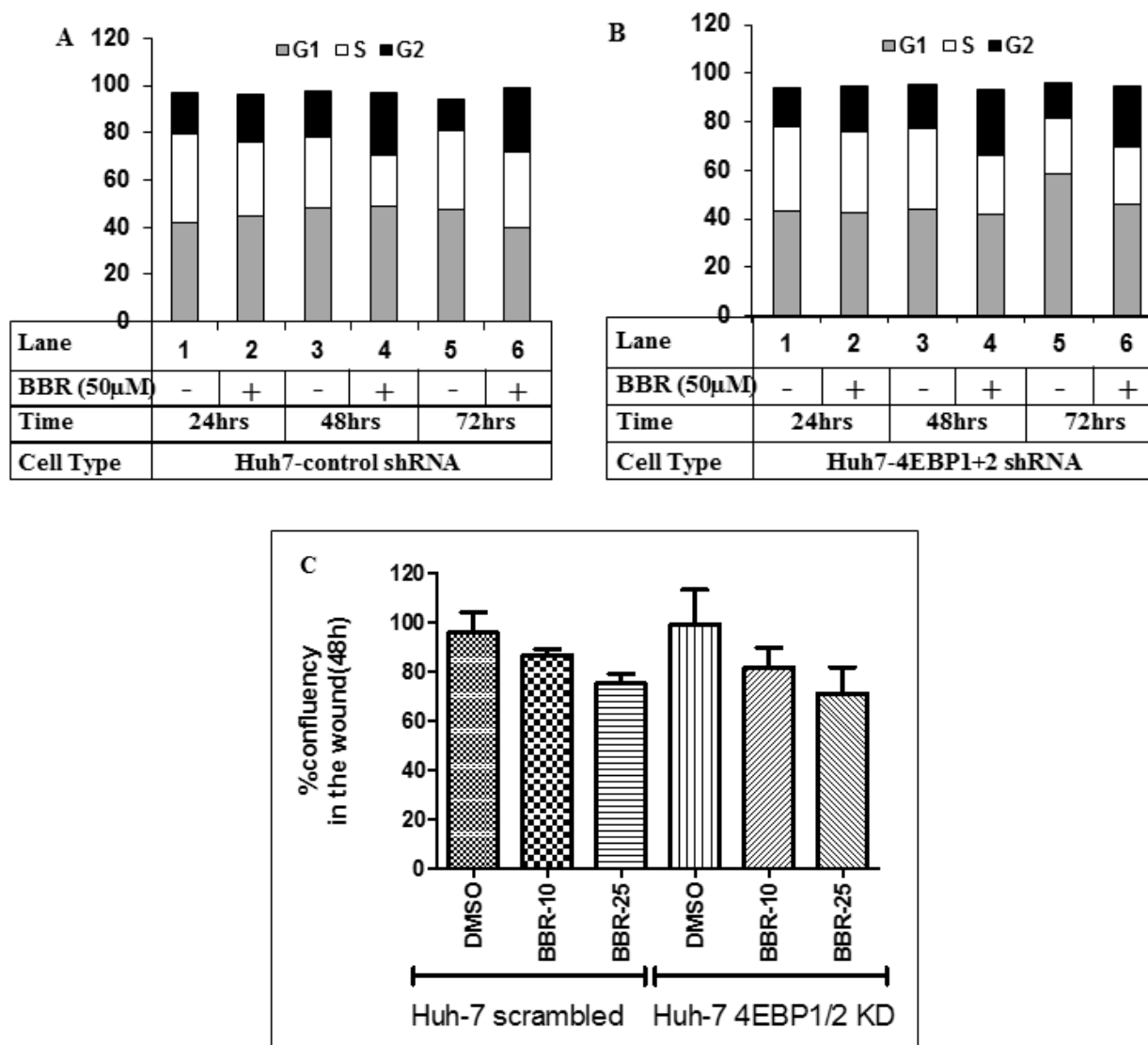
**Supplemental Figure 3: Effect of BBR on β-catenin phosphorylation:** (A) Hep3B and (B) Huh7 cells were treated with vehicle (-) or BBR-50μM (+) for the indicated periods of time and analyzed by westerns blots.



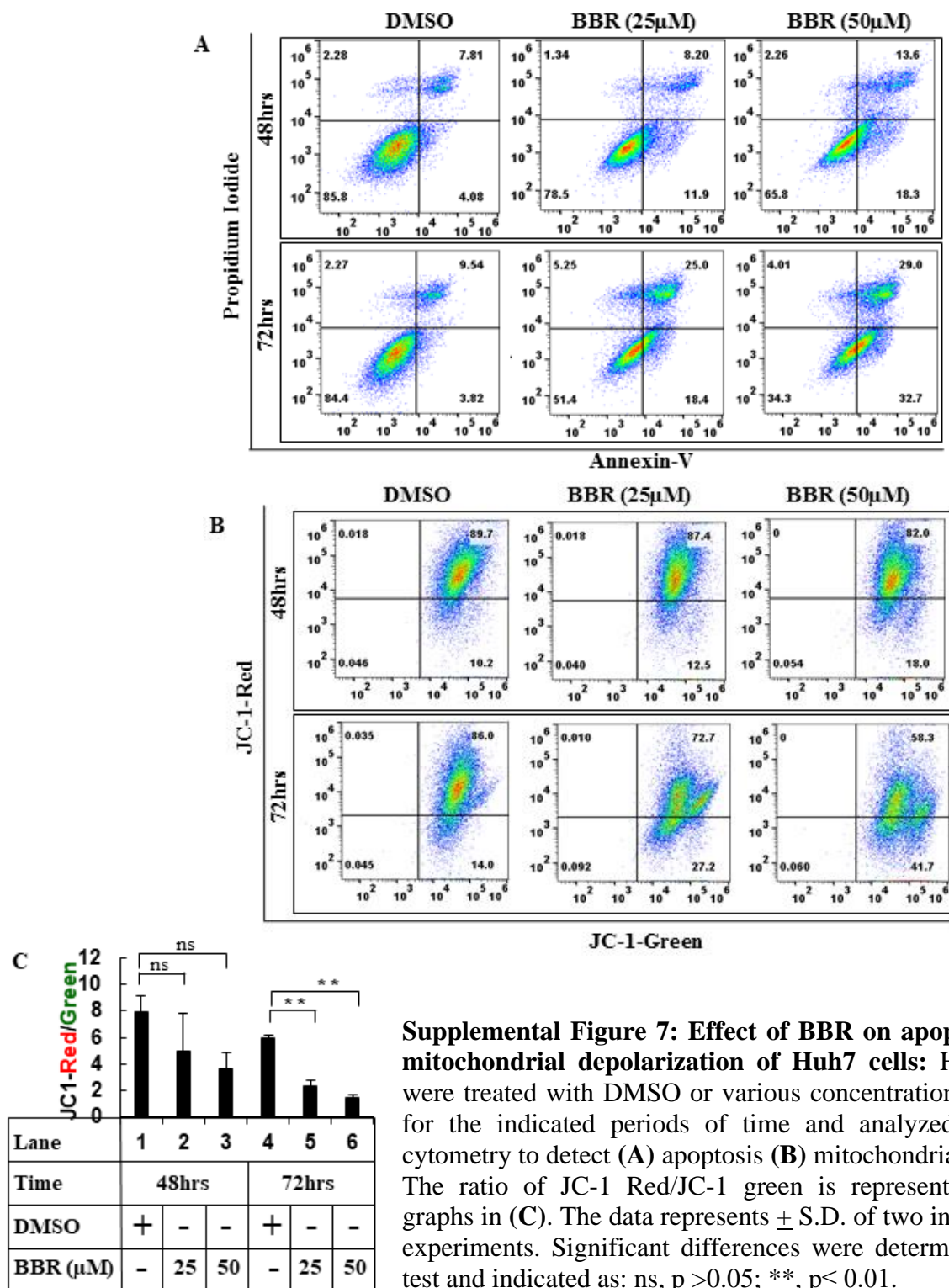
**Supplemental Figure 4: Effect of 4EBP1+2 knockdown on BBR reduction of  $\beta$ -catenin/TCF transcriptional activity:** Huh7-control-shRNA (A) & 4EBP1+2-shRNA cells (B) transiently transfected with pGL3-OT were treated with DMSO or BBR for 24hrs in the presence of control conditioned media (CM) or Wnt3a-CM. Luciferase and  $\beta$ -Gal assays were performed as in Fig 3D. Significant differences were determined by *t*-test and indicated as: ns,  $p > 0.05$ ; \*\*,  $p \leq 0.01$ ; \*\*\*  $p \leq 0.001$ .

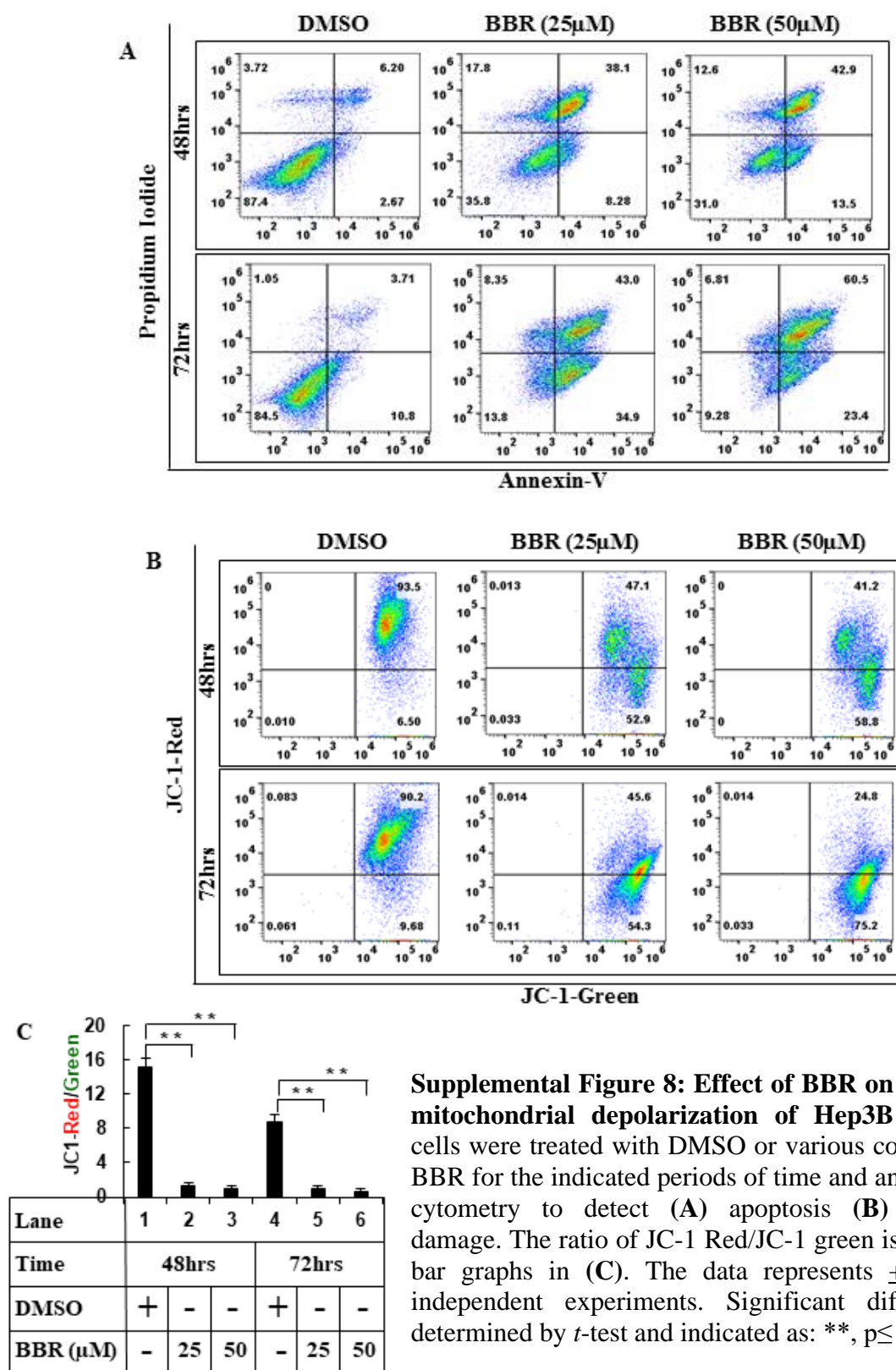


**Supplemental Figure 5: Effect of 4EBP1+2 knockdown on BBR reduction of  $\beta$ -catenin target genes:** Total RNA extracted from Huh7-control-shRNA or -4EBP 1+2-shRNA cells treated with DMSO or BBR for 48hrs were analyzed by qPCR for cyclin D1 (A) and c-Myc (B) gene expressions. The experiments were repeated twice and data represent the mean  $\pm$  S.D. of two independent PCR reactions. Significant differences were determined by *t*-test and indicated as: ns,  $p > 0.05$ ; \*,  $p \leq 0.05$ ; \*\*,  $p \leq 0.01$ .

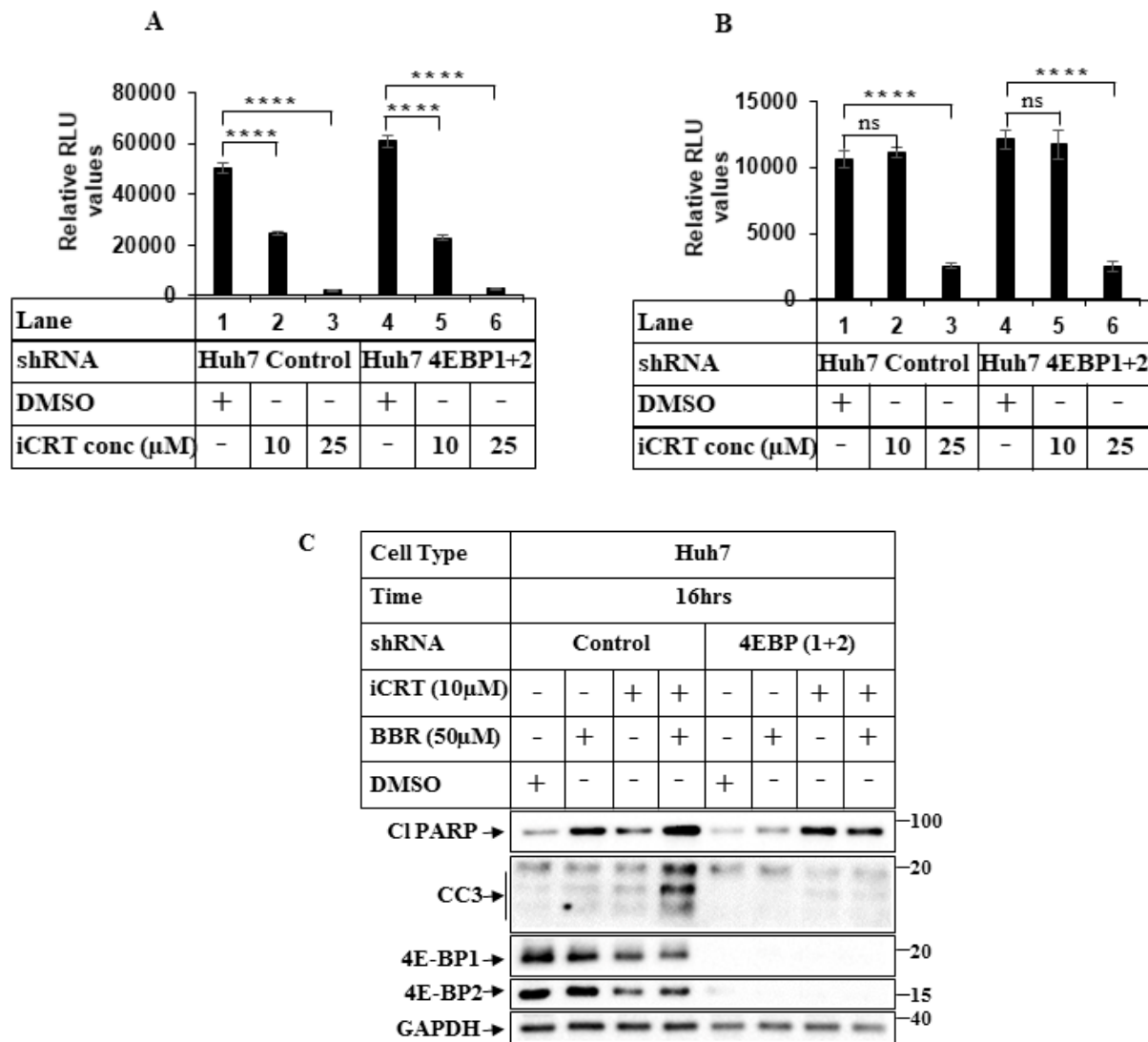


**Supplemental Figure 6: Effect of 4EBP1+2 knockdown on BBR-induced cellular events:** Subconfluent (A) Huh7-control-shRNA or (B) Huh7-4EBP1+2-shRNA cells were serum starved for 24hrs, followed by treatment with DMSO (-) or BBR (+) for the indicated periods of time. Cell cycle analyses were performed by flow cytometry. Data represent average of two independent experiments. (C) Huh7- control-shRNA or -4EBP1+2-shRNA cells plated in 96 well plates (in quadruplicates) and treated with vehicle (DMSO) or BBR (10µM or 25µM) for 48hrs were subjected to migration assay following protocol described under “Materials and Methods”.





**Supplemental Figure 8: Effect of BBR on apoptosis and mitochondrial depolarization of Hep3B cells:** Hep3B cells were treated with DMSO or various concentrations of BBR for the indicated periods of time and analyzed by flow cytometry to detect (A) apoptosis (B) mitochondrial damage. The ratio of JC-1 Red/JC-1 green is represented as bar graphs in (C). The data represents  $\pm$  S.D. of two independent experiments. Significant differences were determined by *t*-test and indicated as: \*\*,  $p \leq 0.01$ .



**Supplemental Figure 9: Effect of iCRT-14 on  $\beta$ -catenin/TCF transcriptional activity:** Huh7-control-shRNA and Huh7-4EBP 1+2-shRNA cells were transiently transfected with pGL3-OT (A) and pGL3-OF (B), followed by treatment with DMSO or two different doses of iCRT-14 for 24hrs. Luciferase and  $\beta$ -Gal assays were performed as in Fig 3D. Significant differences in (A) and (B) were determined by *t*-test and indicated as: ns,  $p > 0.05$ ; \*\*\*\*  $P \leq 0.0001$ . (C) **Effect of iCRT-14 and BBR combination on caspase 3 cleavage:** Huh7-control-shRNA and Huh7-4EBP 1+2-shRNA cells were treated with iCRT-14 or BBR alone or in combination for 16hrs, followed by western blot analysis.